Editorial

〔Lab Med Int 2024; 3(2): 23-24〕

Done is better than perfect. Mark Elliot Zuckerberg

*†Tatsuo Shimosawa, MD., PhD**

†Correspondence: Department of Clinical Laboratory, International University of Health and Welfare, 852 Hatakeda, Narita, Chiba 286-8520, Japan. E-mail: tshimo-tky@umin.ac.jp

* Department of Clinical Laboratory, International University of Health and Welfare Faculty of Medicine.

See article volume 3(2): 42-49

Do you remember when cellular phone started popular? First several decades, it was banned to use in hospital because of the risk on malfunctioning medical devices. But nowadays, no one can survive without cellular phone or connection with web information through internet. Most of the health-care facilities now turn to allow the visitors to use cellular phones. Not only visitors but workers there also use them routinely to communicate each other, search for updated medical information, and for relaxing themselves.

Besides cellular phone as a connection device, starting from year 2000, cellular phone with camera has launched and received high reputations from users and first several years, developers spend a lot of times to install high quality camera on the phone. These days, quality of camera on those phones are high enough and it is a matter of fact for consumers that cellular phone has good quality camera and only few choose phones according to camera quality in Japan [1].

In medical fields, automation devices development rapidly progressed and now artificial intelligence is coming into medical field as well. Those updated tools help the medical workers to save their labor and time as well as make their activities more accurate and rapid. It is needless to say that manual analysis of serum chemistry can not be done in medical facilities. The importance of accuracy is well accepted idea among us. In the field of camera, to reproduce realistic and consistent images from the real world, supreme color accuracy is required. Color accuracy is often assessed using standardized color charts. It is measured by quantifying the difference between the displayed colors and the reference colors. High accuracy can be achieved by several factors such as white balance and saturation the color gamut, sensor characteristics, lens quality, calibration. In the point view of human vision, visuality is very complexed and studied for long. In color perception, the human visual system features only three types of cones cells with their respective color pigments plus light-receptive rod cells for scotopic vision. In addition, it is the human brain that compensates for variations of light wavelengths and light sources in its perception of color. Metamers are pairs of different light spectra perceived as the same color by the human brain. Interestingly, colors that are interpreted as the same or similar by a human are sometimes readily distinguishable by other animals, most notably birds. Moreover, ageing has impact on visual perception. Aging results in the changes of the crystalline lens and cornea, and the pupil size. Advancing ages induces shorter wavelengths of visible light are absorbed, and blue hues appear darker. As a consequence, elderly individuals often experience difficulty discriminating between colors that differ primarily in their blue content, such as blue and gray or red and purple. Blood chemistry exams, we use devices to measure light wave length to quantify the measurements. However, in semiquantitative urinalysis by test-strip, we evaluate them by our eyes which is largely affected by the circumstances of examination room, examiners age as well as their experience. In the current issue, Inagaki and his colleagues reported [2] a novel easy to access method to semi-quantify the color changes of urine test-strip by using cellular phone.

The technique itself is not new and some applications are already developed [3], however, they require a deep learning which implies when insufficient data or false data are input to the device they will make false decision. Inagaki et al. developed a new method which does not require a deep learning and just measure the difference between the displayed colors and the reference colors

which is often used for qualifying camera accuracy. As Mr. Zuckerberg pointed out, any new technique is not perfect but worth developing. Inagaki's method is evaluated under strict condition of light condition and most of the examinations are reliable. Under those condition it can replace the human-based examination or large expensive machines, however, urine strip test is easy, safe and cost-effective screening test for health checks. It can be and should be done as a POCT at home. So far there remains three major issues to be clarified. One is that how quick the cellular phone returns the result. What is the TAT? Current machines and human observation require a few seconds to get the results. It may take few more minutes to record the results but in total, TAT is less than 2 minutes.

The second issue is the condition-dependency. As pointed out above, the current report used very strict condition with a special box to control lights but to use the method widely, the examination can be performed and achieve high quality under loose condition.

Finally, the data show that special gravity was not accurately evaluated neither by human visual exam nor Inagaki's method. The color change does not match the sample 7 step colors in the test-strip is one possible reason and it would require to make more precise sample color chart (current widely use strip apply steps every 0.005)[4] or innovate the method to evaluate color differences. Furthermore test strip method has serious limitation in measurement of specific gravity. Test strip measures only cation by detecting changes of pH by urinary electrolytes such as Na, K and others those react with polyelectrolyte, phosphate buffer or metachromagy in methylene blue and dextran sulphate sodium. Therefore urinary strip does not react with non-electrolytes solute such as urea or creatinine and lower than the true gravity measured by refractometer which measures total solute. We should acknowledge the limitation of strip test in evaluation of specific gravity of urine.

Disclosure

T.S. is an advisor of Sekisui Medical Co., Ltd.

References

1) https://www.soumu.go.jp/johotsusintokei/whitepaper/ja/h24/html/nc122320.html (in Japanese), access June 18, 2024.
2) Inagaki K, Nakamura K. Verification of individual differences in visual judgement of urine test strips and proposal of objective evaluation method. LMI 2024; 3 (2) : 42-49.
3) Flaucher M, Nissen M, Jaeger KM, Titzmann A, Pontones C, Huebner H, Fasching PA, Beckmann MW, Gradl S, Eskofier BM. Smartphone-Based Colorimetric Analysis of Urine Test Strips for At-Home Prenatal Care. IEEE J Transl Eng Health Med. 2022 May 30; 10: 2800109. doi: 10.1109/JTEHM.2022.3179147.
4) JCCLS Document GP3-P1 proposed Guideline Urinary Reagent Strip Method 2001; 16: 33-55 https://www.jccls.org/pdf/approval/063_026.pdf.

Editorial

〔Lab Med Int 2024; 3(2): 25〕

Novel Biomarker in the Diagnosis of Acute Aortic Dissection

*†Naoyuki Yokoyama, MD**

†Correspondence: Department of Medicine, Teikyo University School of Medicine, 2-11-1, Kaga, Itabashi-ku, Tokyo 173-8605, Japan. E-mail: nao-ykym@kc5.so-net.ne.jp

* Department of Medicine, Teikyo University School of Medicine.

See article volume 3(2): 50-58

Acute aortic dissection (AAD) is caused by a tear in the intimal lining of the aorta that extends into the media of the wall [1]. Blood in the aortic media then pushes the dissection flap into the middle of the aorta, separating the true from the false lumen. AAD is a serious condition that can result in significant mortality and morbidity. Aortic dissection mortality increases by 1%–2% per hour after symptom onset. In many cases, immediate intervention is required. Thus, prompt diagnosis is mandatory.

Although imaging is the key tool in the diagnosis of AAD, the assessment of biomarkers is under investigation as a potential rapid diagnostic approach. The following are recognized as the most common biomarkers: white blood cell count, D-dimer, fibrinogen, and C-Reactive Protein (CRP). In particular, D-dimer has high sensitivity for the diagnosis of AAD [2] and is therefore useful for ruling out AAD. However, there are limitations, such as cases of false lumen occlusion and younger patients with AAD, where D-dimer levels remain normal. Additionally, the cutoff value for D-dimer varies depending on the laboratory analytical reagent, so it is necessary to check the cutoff value at each hospital.

This study by Higuchi and colleagues is the first report to analyze the kinetics of citrullinated fibrinogen (C-Fbg) in AAD [3]. C-Fbg is produced when proteins such as fibrinogen are converted by peptidylarginine deiminase in neutrophils during inflammation. It is expected that the pathogenesis of AAD is related to the mechanism of C-Fbg elevation. In this exploratory study, the authors aim to assess whether blood C-Fbg levels are significantly elevated in AAD and whether they differ from those observed in acute coronary syndromes. In this study, C-Fbg showed a significant correlation with D-dimer. It was also found that while D-dimer decreased in blood concentration over time, C-Fbg remained high. These findings suggested that C-Fbg might contribute to the early diagnosis of AAD.

Additionally, an interesting finding of this study is that C-Fbg did not correlate with CRP. C-Reactive Protein (CRP) is an acute-phase reactant produced by the liver in response to cytokines. CRP is an independent risk factor for vascular inflammation and a prognostic factor for cardiovascular events [4]. It has also been confirmed that C-Fbg increases in inflammatory diseases such as rheumatoid arthritis. Based on this report, clinical application to inflammatory aortic syndrome is expected.

References

1) LeMaire SA, Russell L. Epidemiology of thoracic aortic dissection. Nat Rev Cardiol 2011; 8(2): 103-13.
2) Yao J, Bai T, Yang B, Sun L. The diagnostic value of D-dimer in acute aortic dissection: a meta-analysis. J Cardiothorac Surg 2021; 16(1): 343.
3) Fujimura S, Higuchi Y, Izawa et al. Evaluation of serum citrullinated fibrinogen in patients with acute aortic dissection. LMI 2024; 3(2): 50-58.
4) Kaptoge S, Di Angelantonio E, Pennells L, et al. C-reactive protein, fibrinogen, and cardiovascular disease prediction. N Engl J Med 2012; 367(14): 1310-20.

Editorial

〔Lab Med Int 2024; 3(2): 26-27〕

The effect of ISO 15189 implementation for the reduction of incidents

Ririka Miura[*1], Rikei Kozakai*[*1], †Shinichiro Takahashi, MD, PhD*[*1, 2]*

†Correspondence: Division of Laboratory Medicine, Faculty of Medicine, Tohoku Medical and Pharmaceutical University, 1-15-1 Fukumuro, Miyagino-ku, Sendai 983-8536, Japan. E-mail: shintakahashi@tohoku-mpu.ac.jp
Received January 10, 2024; accepted March 16, 2024
*1 Department of Clinical Laboratory, Tohoku Medical and Pharmaceutical University Hospital, 1-12-1 Fukumuro, Miyagino-ku, Sendai 983-8512, Japan
*2 Division of Laboratory Medicine, Faculty of Medicine, Tohoku Medical and Pharmaceutical University, 1-15-1 Fukumuro, Miyagino-ku, Sendai 983-8536, Japan

See article volume 3(1): 8-14

The way to strengthen medical safety have been attracting attention to deliver definite and accurate clinical laboratory data to physicians[1,2]. ISO 15189 is an international standard that specifies the quality management system (QMS) requirements particular to medical laboratories, and ISO 15189 has been reported to play an important role in quality improvement and prevention of examination errors[3-8].

Recently, we reported about our experience for the effect of ISO 15189 implementation for the reduction of the number of incidents[4]. We experienced that the total number of incidents decreased significantly even one year after accreditation. In the literature search, similar observations were reported[5-8], and in this Editorial, we are going to introduce these papers describing the effect on the reduction of the number of incidents after accreditation of ISO 15189.

First paper is from Yoshiko et al[5], from Nagoya University Hospital. They acquired ISO 15189 accreditation in November, 2009. They revealed that post-accreditation, the number of nonconformities and incident reports were decreased. They revealed that the number of incidents were decreased from 100 in 2009, to 94 in 2010. They also revealed that the level 0 and level 1 incidents increased in 2010 (level 0, 13% in 2009 to 18.3% in 2010; level 1, 48% in 2009 to 53.8% in 2010), whereas level 2 and level 3a incidents decreased in 2010 (level 2, 32% in 2009 to 24.7% in 2010; level 3a, 2% in 2009 to 1.1% in 2010), also suggesting that ISO 15189 works well for reduction of number and level of incidents. Additionally, they pointed out some problems related to the post accreditation of ISO 15189, which is the increment of the complaints from the staffs and increase of overtime works to operate QMS[5].

Next paper is from Shitara et al[6], from Kosei general hospital. They acquired ISO 15189 certification on December 1, 2005. Although they did not investigate the level of the incidents precisely, they revealed the total number of incidents decreased obviously (year, cases; 2003, 57; 2004, 65; 2005, 26; 2006, 25; 2007, 24)[6]. They also found that, more than 80% of the incidents occurred through 2003 to 2007 were from "5.4 pre-examination processes", "5.5 examination processes", and "5.8 reporting of results" in the standard requirements of ISO 15189, and the proportions have not been changed throughout this period[6]. In addition, the proportions of incidents in each process were relatively similar to those in a previous report[9].

Third paper is from Ota et al.[7], from St. Mary's hospital. They acquired ISO 15189 authorization in December 2007. They revealed that total incidents in 2007 was 240 cases whereas 62 cases in 2010, which is three years after accreditation[7]. What was characteristic in their report was, in the process of authorization acquisition, they tried to improve ward nursing management using ISO 15189, drew up standard operating procedures through detailed job analysis, and enabled ward operation standardization[7].

Last paper is from Okada et al.[8], from Okayama University hospital. They got ISO 15189 accreditation on July, 2007. In the year of 2005, two years before their accreditation, the total number of incidents was 116. Then the

number was decreased to 84, in 2006 and 2007, and finally dropped to 48, a year after accreditation. They concluded that the frequency of laboratory incidents was reduced through seeking the causes of incidents and performing continual improvement according to ISO 15189: "Plan, Do, Check, Act". They also described that the motivation and competence of laboratory staff concerned have also improved, consequently leading to a favorable influence on other laboratory staff members.

Collectively, all of these published five papers clearly demonstrate that implementation of a QMS meeting ISO 15189 standards is effective for the reduction of incidents. As far as we searched, no paper has been found for the negative effect of ISO 15189 on medical safety. The effect of this implementation may take several years for the sufficient effect for the reduction of incidents. Recently, ISO 15189:2012 has been updated to ISO 15189:2022, with increased emphasis on risk management[10]. All of reports presented in this paper are based on ISO 15189:2012, or earlier, version of ISO 15189. Therefore, we are now expecting that implementation of this new ISO 15189:2022 QMS will further improve measures for medical safety.

References

1) Tsunekawa K, Asai Y, Ikegami S, et al. Incident analysis and preventive measures taken in the general laboratory of hospital. Jap J Med Tech 2019; 68 (2): 333-8.
2) Maeda F, Izumi S, Nakanishi H, et al. Efforts of inspection technology department and medical safety management committee: lncident accident report, positive report, fiscal year safety target. Jap J Med Tech 2017; 66 (4): 404-10.
3) Kayamori Y, Fujishima A, Noda (Inoue) N, et al. Approach for prevention medical test malpractice using ISO 15189. Rinsho Byori 2010; 58 (8): 839-46.
4) Miura R, Kozakai R, Suzuki S, et al. Analysis of Incident/Accident Reports in the Department of Clinical Laboratory at Tohoku Medical and Pharmaceutical University Hospital: Effect of ISO 15189 Implementation on Medical Safety. Lab Med Int 2024; 3 (1): 8-14.
5) Yoshiko K. Effects of the ISO 15189 Accreditation on Nagoya University Hospital. Rinsho Byori 2012; 60 (7): 667-73.
6) Shitara M, Umezu S, Katsuno H. Effects of the ISO 15189 Accreditation on Clinical Laboratory. Rinsho Byori 2009; 57 (6): 521-6.
7) Ota Y, Ide H, Tsukamoto T, et al. From the Position of a Private Sector Hospital: ISO 15189 Acquisition by a Clinical Laboratory, and Quality Management System Deployment in the Whole Hospital. Rinsho Byori 2012; 60 (7): 677-82.
8) Okada K, Itoshima K, Watanabe T, et al. Effect of ISO 15189 accreditation on Okayama University Hospital. Rinsho Byori 2009; 57 (10): 971-7.
9) Astion ML, Shojania KG, Hamill TR, et al. Classifying laboratory incident reports to identify problems That Jeopardize Patient Safety. Am J Clin Pathol 2003; 120 (1): 18-26.
10) ISO 15189: 2022. Medical laboratories–requirements for quality and competence. Geneva: International Organization for Standardization; 2022.

Case Report

Thyroid storm with elevated presepsin without infection due to methimazole administration

*†Tetsuo Hayakawa*1, Keisuke Kurokawa*2, Ken-Ichiro Kato*1*

†Correspondence: Department of Diabetes Mellitus and Endocrinology, Tonami General Hospital, 1-61 Shintomi-Cho, Tonami, 939-1395, Japan.
E-mail: thayakawaendo@gmail.com
*1 Department of Diabetes Mellitus and Endocrinology, Tonami General Hospital
*2 Department of Cardiology, Tonami General Hospital

ABSTRACT

A 43-year-old woman was diagnosed with thyroid storm due to Graves' disease. Fever and inflammatory reactions were observed; however, the infectious focus was unclear. The patient was administered methimazole, potassium iodide, and meropenem. The presepsin levels increased and the fever persisted, but the C-reactive protein and procalcitonin (PCT) levels decreased. The meropenem and methimazole were discontinued, and propylthiouracil was initiated. The patient's presepsin levels and thyroid function decreased; however, her fever continued. A total thyroidectomy was performed, and the patient's fever improved while her presepsin and PCT levels normalized. Treatment with methimazole during thyroid storm may result in the secretion of presepsin without infection, which must be considered when diagnosing sepsis in patients with thyroid storm.

〔Lab Med Int 2024; 3(2): 28-32〕

Key Words
presepsin, procalcitonin, thyroid storm, methimazole

I. Introduction

Thyroid storm is a life-threatening endocrine emergency that originates from thyroid toxicosis. The condition manifests as the decompensation of multiple organs with a high fever, disturbed consciousness, heart failure, diarrhea, and jaundice [1]. Patients with thyroid storm and fever must be monitored carefully as severe thyroid storm may be complicated by pneumonia or urinary tract infections [2].

Presepsin and procalcitonin (PCT) are novel diagnostic and prognostic markers for sepsis. Presepsin is considered a promising biomarker for diagnosing sepsis and can be detected during sepsis earlier than C-reactive protein (CRP) and PCT [3].

This report presents a patient with thyroid storm who was treated with methimazole and experienced an increase in her plasma presepsin level without infection.

II. Case report

A 43-year-old woman was admitted to our hospital for thyroid toxicosis with a temperature of 39.2℃, blood pressure of 131/59 mmHg, heart rate of 145 /min, and nausea. Acute physiology and chronic health evaluation (APACHE) II score and sequential organ failure assessment (SOFA) score were 12 and two points, respectively. The thyroid gland was slightly enlarged. Ultrasonography of the thyroid gland revealed a heterogeneous internal echo with slightly increased blood flow (**Figure 1**). The TSH receptor antibody (TRAb) and thyroid stimulating antibody (TSAb) were elevated (5.1% and 685%, respectively). The patient was diagnosed with thyroid storm due to Graves' disease. The clinical course of the patient is shown in **Figure 2**. She was administered methimazole (60 mg/day), potassium iodide (0.2 g/day), landiolol (1 μg/kg/min for a total of 68 mg/day), hydrocortisone (200 mg/day for hospital days 1-3), and acet-

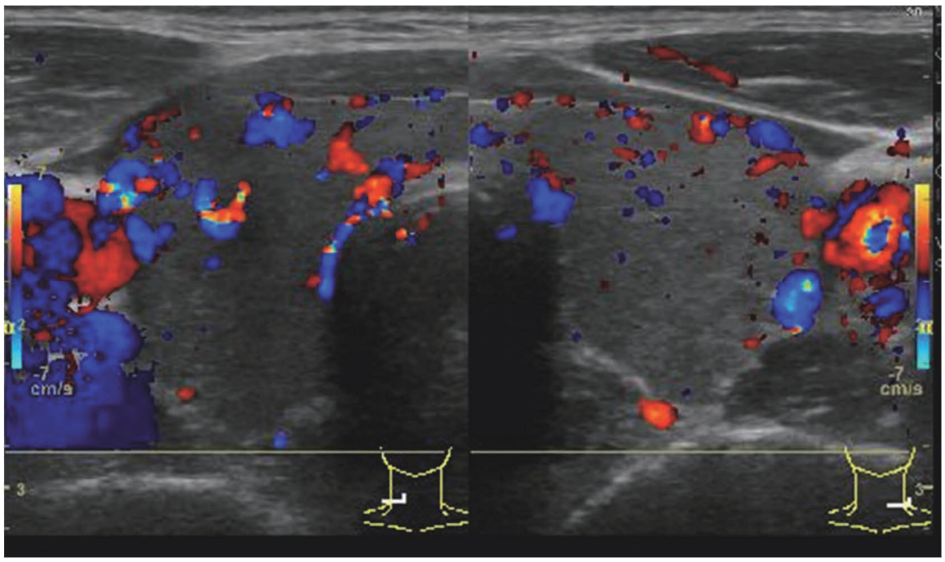

Figure 1 Ultrasonography of the thyroid gland showing heterogeneous internal echo and slightly increased of blood flow.

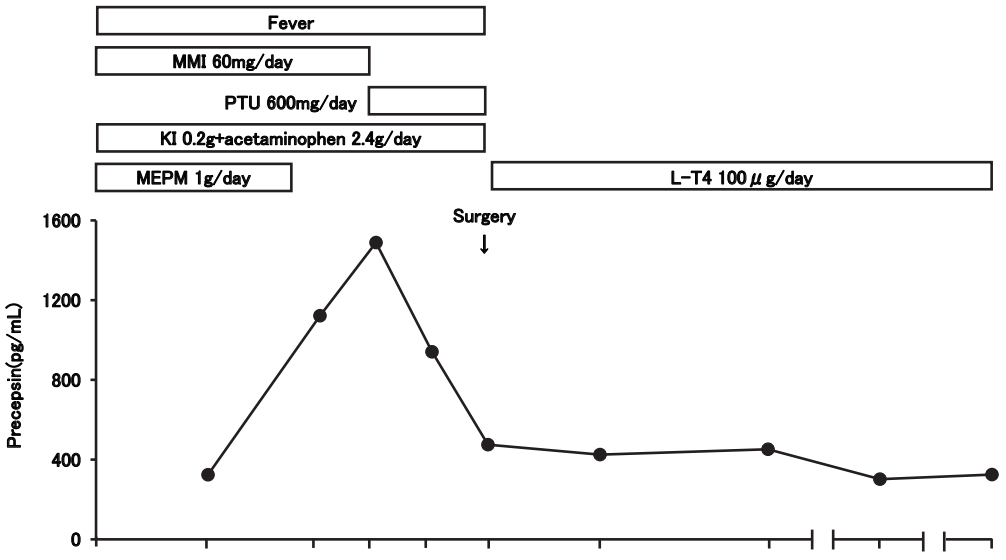

(Day)	1	9	16	20	23	27	35	44	65	93
PCT (ng/mL)	0.63	0.11	0.06	0.09	0.11	0.09	0.06	0.06	0.07	<0.05
CRP (mg/dL)	11.55	3.20	3.63	5.06	4.55	4.53	3.20	3.00	3.79	2.97
WBC (/μL)	10600	12700	10000	11000	7300	7600	7500	6600	5500	5200
FT3 (pg/mL)	14.6	4.6	5.4	7.3	5.1	2.4	1.1	1.0	1.2	1.8
FT4 (ng/dL)	9.3	2.0	2.3	3.2	2.4	1.5	0.5	0.4	0.6	1.2
TSH (μIU/mL)	<0.02	<0.02	<0.02	<0.02	<0.02	0.02	<0.02	0.77	20.32	7.53
ALP (U/L)	619	473	833	935	741	777	834	703	593	960
γ-GTP (U/L)	84	64	153	166	135	149	191	143	141	155
T.Bil (mg/dL)	1.3	0.4	0.4	0.5	0.3	0.3	0.5	0.4	0.4	0.3
eGFR (mL/min/1.73m^2)	90.1	79.4	106.3	104.0	99.6	95.6	91.9	88.4	82.2	86.8

Figure 2 Clinical course. Day 1 indicates admission. KI=potassium iodide, MEPM=meropenem, MMI=methimazole, PCT=procalcitonin, PTU=propylthiouracil.

aminophen (2.4 g/day). The patient's inflammatory responses, such as white blood cell (WBC) count and CRP and PCT levels, were also elevated. The blood cultures were negative. Whole-body computed tomography (CT) and echocardiography were conducted; however, the infection focus remained unclear. Thyroid storm complicated by bacterial infection was suspected, and meropenem (1 g/day) was administered. Palpitation and nausea improved immediately, but the fever persisted. The patient's CRP, PCT, and T.Bil levels decreased, but the presepsin, ALP, and γ-GTP levels increased. Renal function, AST, and ALT levels were within normal ranges. The infection focus was unclear on gallium scintigraphy and repeated whole-body CT. The blood culture results were negative. It was believed that the bacterial infection improved. The meropenem was discontinued on hospital day 12. The patient's CRP and PCT levels continued to decrease; however, her presepsin, ALP, and γ-GTP levels increased, and the fever continued. On hospital day 20, the methimazole was discontinued and propylthiouracil was initiated due to the possibility of fever secondary to methimazole. The patient's presepsin, ALP, and γ-GTP levels decreased. Thyroid function decreased, but her fever continued. It was believed that the fever was due to thyroid storm, and a total thyroidectomy was performed on hospital day 27. Histopathological features revealed fibrotic tissues, and the follicular epithelia exhibited local hyperplasia and papillary proliferation. Scalloping, formed by vacuoles in the colloid adjacent to the apex of the follicle cells, was increased locally. Lymphocytic infiltration with follicular formation was observed in the interstitial tissues. These findings are consistent with Graves' disease after treatment (**Figure 3**). The patient's fever resolved immediately after thyroidectomy. The presepsin and PCT levels normalized one and two months after surgery, respectively.

III. Discussion

Fever is reported in 63.5-64.9% of Japanese patients with thyroid storm [1]. The irregular use or discontinuation of antithyroid drugs and infections account for 44.7% and 31.4% of cases of thyroid storm, respectively [1]. Upper respiratory tract infections, acute bronchitis/pneumonia, and agranulocytosis/sepsis account for 41.5%, 20.7%, and 3.7% of the infections leading to thyroid storm, respectively [4].

In this patient, thyroid storm complicated by bacterial infections was suspected upon admission due to the patient's WBC count and CRP and PCT levels. The bacterial infection was believed to improve during the treatment as the CRP and PCT levels decreased; however, the presepsin levels increased. The patient's meropenem was discontinued and the methimazole was changed to propylthiouracil; however, the fever continued. The fever was believed to be due to the thyroid storm, and a total thyroidectomy was performed.

Presepsin is a 13-kDa protein that is the truncated N-terminal fragment of CD14 and is highly expressed on the membrane surfaces of monocytes [5]. Presepsin secretion by monocytes is triggered by bacterial phagocytosis or sterile phagocytic stimuli. Elastase in monocytes mediates CD14 cleavage to produce presepsin [6]. Presepsin levels are significantly elevated in patients with sepsis and hemophagocytic syndrome [6-8]. Presepsin levels may also increase with an increase in macrophage phagocytic activity. In a previous report, a patient with Graves' disease developed agranulocytosis and hemophagocytic syndrome after the administration of methimazole [9]; however, the patient's presepsin levels were not reported. PCT is secreted from multiple tissues during bacterial infec-

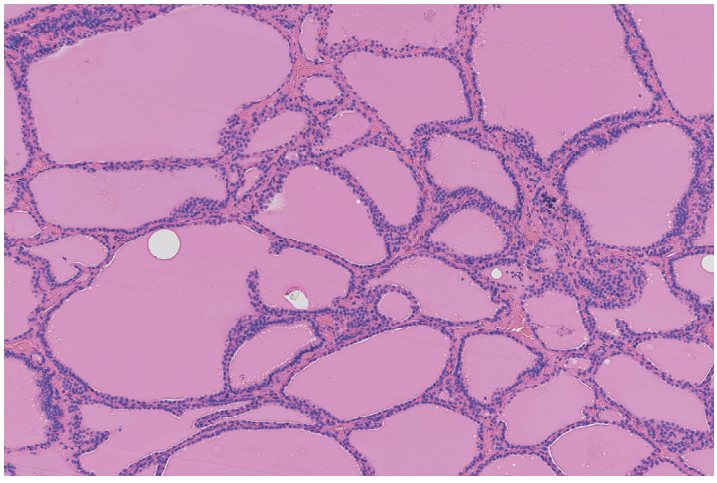

Figure 3 Histopathological features of thyroid specimen shown by hematoxylin and eosin staining (× 100).

tion, including the liver, kidneys, lungs, intestines, and muscles [10]. In the current patient, fever was observed without splenomegaly, cytopenia, hypertriglyceridemia, or hypofibrinogenemia. As the bone marrow, ferritin levels, and soluble interleukin-2 receptor levels were not examined, hemophagocytic syndrome could not be diagnosed.

Presepsin levels were correlated with the elevation of biliary enzymes in patients without renal dysfunction or sepsis. Presepsin production in liver Kupffer cells was confirmed by immunostaining [11]. These findings suggest that increased bile duct pressure results in presepsin over expression in the Kupffer cells, leading to elevated presepsin levels in both the bile and plasma [11]. In this patient, ALP and γ-GTP levels increased after the administration of methimazole, and decreased when methimazole was changed to propylthiouracil. It is possible that presepsin level increased due to the increase of bile duct pressure by methimazole; however, as we did not perform immunostaining of presepsin in the liver, this could not be proven. The frequency of severe liver injury, such as hepatic coma and hepatic failure, or mild liver injury to the use of methimazole was 0.05% or 0.09%, respectively. The frequency of severe or mild liver injury to the use of propylthiouracil was 0.17% or 0.04%, respectively [12]. Liver injury associated with methimazole is related to cholestasis, whereas the liver injury associated with propylthiouracil is related to hepatitis [12].

Presepsin levels have been shown to be significantly increased in patients with renal dysfunction [13,14]. As presepsin is a 13-kDa protein, it is freely filtered by the glomerulus and almost completely reabsorbed and catabolized with proximal tubular cells [14]. In this patient, renal function was within the normal range.

Presepsin is correlated with disease activity in patients with systemic lupus erythematosus (SLE), for which several reasons have been proposed [15]. The clearance ability of apoptotic body/cellular debris and neutrophil phagocytosis are impaired in these patients and the cathepsin D activity and neutrophil extracellular cell trap production are increased. In patients with thrombocytopenia, anasarca, fever, reticulin fibrosis, and organomegaly (TAFRO) syndrome, the presepsin and alkaline phosphatase levels are increased [16]. Presepsin and troponin levels are significantly elevated in patients with acute myocardial infarction (AMI) [17]. However, the mechanisms underlying increased presepsin levels in patients with TAFRO syndrome and AMI are not well known.

In this patient, the presepsin level decreased when methimazole was changed to propylthiouracil. Treatment with methimazole during a thyroid storm may lead to presepsin secretion via a sterile phagocytic stimulus or an increase of bile duct pressure. We did not perform immunostaining of presepsin in the liver or thyroid gland. The precise mechanism underlying the methimazole-induced increase in presepsin levels is unclear. Further studies are needed to elucidate the mechanism by which methimazole increases the presepsin level in patients with thyroid storm without infection.

Conflict of Interest

The authors declare that they have no conflicts of interest.

References

1) Akamizu T, Satoh T, Isozaki O, et al. Diagnostic criteria, clinical features, and incidence of thyroid storm based on nationwide surveys. Thyroid 2012; 22 (7) : 661-79.
2) Satoh T, Isozaki O, Suzuki A, et al. 2016 Guidelines for the management of thyroid storm from The Japan Thyroid Association and Japan Endocrine Society (First edition). Endocr J 2016; 63 (12) : 1025-64.
3) Hung SK, Lan HM, Han ST, et al. Current evidence and limitation of biomarkers for detecting sepsis and systemic infection. Biomedicines 2020; 8 (11), 494: doi:10.3390/biomedicines8110494.
4) The Japan Thyroid Association and the Japan Endocrine Society. 2017 guidelines for the management of thyroid storm. Tokyo: Nankodo; 2017. p.12-3 (in Japanese).
5) Yaegashi Y, Shirakawa K, Sato N, et al. Evaluation of a newly identified soluble CD14 subtype as a marker for sepsis. J Infect Chemother 2005; 11 (5) : 234-8.
6) Arai Y, Mizugishi K, Nonomura K, et al. Phagocytosis by human monocytes is required for the secretion of presepsin. J Infect Chemother 2015; 21 (8) : 564-9.
7) Nanno S, Koh H, Katayama T, et al. Plasma levels of presepsin (soluble CD14-subtype) as a novel prognostic marker for hemophagocytic syndrome in hematological malignancies. Intern Med 2016; 55 (16) : 2173-84.
8) Koh H, Nanno S, Katayama T, et al. Diagnostic usefulness of plasma presepsin (soluble CD14-subtype) for diagnosing hemophagocytic syndrome in hematological malignancies. Leuk lymphoma 2017; 58 (10) : 2489-92.
9) Lew WH, Chang CJ, Lin JD, et al. Successful preoperative treatment of a Graves' disease patient with agranulocytosis and hemophagocytosis using double filtration plasmapheresis. J Clin Apher 2011; 26 (3) : 159-61.
10) Müller B, White JC, Nylén ES, et al. Ubiquitous expression of the calcitonin-I gene in multiple tissues in response to sepsis. J Clin Endocrinol Metab 2001; 86 (1) : 396-404.

11) Yamaguchi T, Ohira M, Kawagoe N, et al. High presepsin concentrations in bile and its marked elevation in biliary tract diseases: A retrospective analysis. Clin Chim Acta 2021; 521: 278-84.
12) Rivkees SA, Szarfman A. Dissimilar hepatotoxicity profiles of propylthiouracil and methimazole in children. J Clin Endocrinol Metab 2010; 95(7): 3260-7.
13) Nagata T, Yasuda Y, Ando M, et al. Clinical impact of kidney function on presepsin levels. PLoS One 2015; 10(6): e0129159.
14) Chenevier-Gobeaux C, Trabattoni E, Roelens M, et al. Presepsin (sCD14-ST) in emergency department: The need for adapted threshold values? Clin Chim Acta 2014; 427: 34-6.
15) Tanimura S, Fujieda Y, Kono M, et al. Clinical significance of plasma presepsin levels in patients with systemic lupus erythematosus. Mod Rheumatol 2018; 28(5): 865-71.
16) Shimizu N, Yamaguchi T, Terai K, et al. A case of TAFRO syndrome who showed remarkable elevation of presepsin level without an apparent infectious disease. JJSLM 2022; 70(1): 29-34 (in Japanese).
17) Caglar FNT, Isiksacan N, Biyik I, et al. Presepsin (sCD14-ST): could it be a novel marker for the diagnosis of ST elevation myocardial infarction? Arch Med Sci Atheroscler Dis 2017; 2(1): e3-8.

Original

Molecular characterization of *Staphylococcus epidermidis* bloodstream isolates from two hospitals in Tokyo

Kayo Yamada[*1†], Alafate Ayibieke, PhD*[*1†], Akari Ikeda*[*1], Kageto Yamada, PhD*[*2], Shinji Ogihara, PhD*[*3], Shuji Tohda, MD, PhD*[*4], †Ryoichi Saito, PhD*[*1]*

†Correspondence: Department of Molecular Microbiology, Graduate School of Medical and Dental Sciences, Tokyo Medical and Dental University (TMDU), 1-5-45, Yushima, Bunkyo-ku, Tokyo 113-8510, Japan.
E-mail: r-saito.mi@tmd.ac.jp
Received February 6, 2023; accepted April 26, 2024
*1 Department of Molecular Microbiology, Tokyo Medical and Dental University Graduate School of Medical and Dental Sciences, Tokyo, Japan
*2 Department of Microbiology and Infectious Disease, Toho University School of Medicine, Tokyo, Japan
*3 Department of Clinical Laboratory, Toho University Medical center Omori Hospital, Tokyo, Japan
*4 Department of Clinical Laboratory, Tokyo Medical and Dental University Hospital, Tokyo, Japan
† These two authors contributed equally to this work.

ABSTRACT

Dissemination of multidrug-resistant *Staphylococcus epidermidis*, especially methicillin-resistant *S. epidermidis* (MRSE), with enhanced pathogenicity is a serious global public health concern. We characterized the antimicrobial/biocide susceptibility and virulence of 105 *S. epidermidis* bloodstream isolates from two hospitals in Tokyo to expand on the limited information available in Japan.

The phenotypic and genetic features of antimicrobial resistance, biocide tolerance, SCC*mec* type, and biofilm development or adhesion were analyzed.

In total, 76 (72.4%) isolates were identified as MRSE, which showed higher resistance rates to most antimicrobial classes, except for vancomycin, than methicillin-susceptible *S. epidermidis* (MSSE). MRSE was classified into 16 sequence types (STs), including the most prevalent ST2, which is a global high-risk *S. epidermidis* clone. In addition, our MRSE isolates possessed higher rates of *qacA/B* than the MSSE isolates, resulting in a higher tolerance to the three low-level antiseptics compared to MSSE isolates. Among these, ST6 and ST2 isolates showed higher *qacA/B* positivity rates. Furthermore, SCC*mec* type IV was predominant in the MRSE isolates. MRSE isolates possessed *aap* and IS*256* more frequently than MSSE isolates. Moreover, *sesI* and *icaA* were found in the ST2 isolates. The proportion of biofilm producers in MRSE tended to be higher than that in MSSE, and strong biofilm producers were concentrated in ST2 isolates among the four predominant STs.

Collectively, our findings provide the first evidence that highly virulent, multidrug-resistant *S. epidermidis* isolates, including the global ST2 MRSE lineage, may have already spread and persisted for a long time in healthcare facilities in Japan.

〔Lab Med Int 2024; 3(2): 33-41〕

Key Words
Staphylococcus epidermidis, methicillin resistance, *mecA*, biocide tolerance, biofilm, sequence type

I. Introduction

Staphylococcus epidermidis is the most common species of coagulase-negative staphylococci (CoNS) and a normal human commensal bacterium in the skin and mucous membranes. Although it is an important opportunistic pathogen, it is also a leading cause of healthcare-associated infections (HAIs) involving medical devices such as catheters and prosthetic joints[1)2)]. In Japan, *S. epidermidis* is the most frequently identified pathogen associated

with catheter-associated bloodstream infections[3].

S. epidermidis can acquire determinants conferring antimicrobial resistance and biocide tolerance, which can be horizontally transferred to other *Staphylococcus* species[1)4)]. The recent emergence and dissemination of multidrug-resistant *S. epidermidis*, especially methicillin-resistant *S. epidermidis* (MRSE) with staphylococcal cassette chromosome *mec* (SCC*mec*), has become a global concern because of the difficulty in treating infections, prolonged hospitalization, and increased healthcare costs[5)]. In addition, *S. epidermidis* has enhanced pathogenicity due to acquired virulence factors, such as biofilm development and adherence, and has been isolated globally[2)6)]. Furthermore, among several global hospital-adapted HAI-associated *S. epidermidis* lineages, sequence type (ST) 2 of clonal complex 2 (CC2) has been one of the most prevalent MRSEs in recent decades [2)5)7)].

Although these factors may have contributed to the MRSE lineage becoming a globally successful clone in healthcare facilities, this phenomenon is not yet fully understood. Despite the frequent isolation of HAIs globally, knowledge regarding the phenotypic and genomic characteristics, such as antimicrobial resistance or virulence, of *S. epidermidis* isolates from Japan is still limited. Therefore, in this study, we aimed to clarify the profiles of antimicrobial and biocidal susceptibilities, biofilm formation, and genetic features, including the SCC*mec* type, of *S. epidermidis* bloodstream isolates from Japan.

II. Methods

A. Bacterial samples and growth conditions

A total of 105 non-duplicate *S. epidermidis* isolates recovered from at least two sets of positive blood cultures per patient, collected between 2007 and 2015 (n = 43) at the Tokyo Metropolitan Toshima Hospital and between 2014 and 2015 (n = 62) at the Tokyo Medical and Dental University Hospital, were used in this study. Microbial identification was confirmed using a MALDI Biotyper (Bruker Daltonics, Karlsruhe, Germany). The *S. epidermidis* strains were grown at 37℃ under aerobic conditions on tryptone soya agar plates and tryptone soya broth (Oxoid, Hampshire, United Kingdom).

B. Antimicrobial susceptibility testing and minimal inhibitory concentrations of biocides

Minimal inhibitory concentrations (MICs) of 12 antimicrobials (penicillin, oxacillin, ampicillin, cefazolin, imipenem, gentamicin, erythromycin, clindamycin, minocycline, levofloxacin, vancomycin, and sulfamethoxazole/trimethoprim), were determined by microdilution using commercial plates (Eiken Chemical, Tokyo, Japan). The detailed MIC of oxacillin in all ST2 isolates was also measured using Etest (bioMérieux Marcy-l'Étoile, France). All the results were interpreted according to the CLSI M100- ED30 guidelines.

Similarly, the MICs of chlorhexidine, benzalkonium chloride, and olanexidine gluconate were determined using the broth doubling microdilution method according to the CLSI M100-ED30 guidelines[8)].

C. Antimicrobial resistance, biocide tolerance, and biofilm development or adhesion genes screening

DNA was extracted using the Cica Geneus™ DNA Extraction Reagent (Kanto Chemical, Tokyo, Japan). *mecA* and seven biofilm development- or adhesion-associated genes (*sesI*, *icaA*, *bhp*, *aap*, *atlE*, *arcA*, and IS*256*) identified in *Staphylococcus* species were screened using PCR as previously described[9)-14)]. PCR screening was also conducted for two major multidrug efflux pump-encoding genes for biocide tolerance: *qacA/B* and *smr*[15)].

D. Multi-locus sequence typing

Multilocus sequence typing (MLST) was performed using seven loci (*arcC*, *aroE*, *gtr*, *mutS*, *pyrR*, *tpi*, and *yqiL*), as previously described[16)], with some modifications. Briefly, *aroE* was amplified with the primers aroE-F2 (5'-TCAGCACCTTGATGAACGAA-3) and aroE-R2 (5'-GAACGTATTATTCCGTACCTAGATG-3). PCR was performed using the 2 × EmeraldAmp MAX PCR Master Mix (Takara Bio, Shiga, Japan), and the products were purified and sequenced. STs were defined using the PubMLST *S. epidermidis* genome database (https://pubmlst.org/organisms/staphylococcus-epidermidis). The minimum spanning tree for genetic relatedness of the MLST data was visualized with goeBURST Full MST using PHYLOVIZ 2.0[17)].

E. PCR-based SCC*mec* typing

PCR-based SCC*mec* typing of 76 MRSE strains was performed according to previously described methods [18)19)], and the SCC*mec* type was interpreted based on the guidelines of the International Working Group on the Classification of Staphylococcal Cassette Chromosome Elements[20)]. When the combined results for *mec* class and *ccr* type were not reported before, or when no *mec* or *ccr* was detected, they were classified as non-typeable.

F. Biofilm formation quantification

Biofilm formation assays were conducted in 96-well polystyrene plates (AS ONE Corporation, Osaka, Japan), as previously described[21)22)], with some modifications. Briefly, 3-h pre-cultured *S. epidermidis* isolates were inoculated into 2 ml fresh 1% glucose containing TSB (OD550 = 0.01–0.04), and then 200 μL of these cultures were transferred into each well, followed by overnight

incubation at 37℃. Following incubation, all liquids were removed and the wells were washed three times with distilled water. The plates were stained with 1% (w/v) crystal violet solution, washed three times, and dried for 10–15 minutes. Finally, 200 μL 99.5% ethanol was added to each well, and the stained biofilms were measured at 570 nm using a MULTISKAN FC (Thermo Fisher Scientific, Waltham, MA, USA). Each isolate was tested at least six times; the mean results are presented.

Biofilm formation was assessed as described previously[23]. Briefly, the isolates were categorized as strong, moderate, weak, or non-biofilm producers according to the following equations:

OD < ODC (average OD of negative control) = non-biofilm producer

ODC < OD ≤ (2 × ODC) = weak biofilm producer

(2ODC) < OD ≤ (4 × ODC) = moderate biofilm producer

(4 × ODC) < OD = strong biofilm producer.

S. epidermidis ATCC 12228, which lacks biofilm formation, was used as a negative control.

G. Statistical analysis

Categorical variables were evaluated using the chi-square test. Statistical differences were determined using the Mann-Whitney U test. $p < 0.05$ was set as the threshold of significance.

III. Results

A. Antimicrobial susceptibility profile and its relationship with *mecA* prevalence

Among 105 *S. epidermidis* isolates, 76 (72.4%) were identified as MRSE, and 29 (27.6%) were identified as methicillin-susceptible *S. epidermidis* (MSSE) (**Table 1**). All MRSE isolates harbored *mecA*, whereas the MSSE isolates did not. The resistance rates to most other antimicrobial classes were significantly higher in MRSE than

Table 1 Antibiotic susceptibility profiles of 105 S. *epidermidis* isolates

Antibiotic	MSSE (n=29)				MRSE (n=76)				p-value
	MIC (μg/mL)			%R	MIC (μg/mL)			%R	
	Range	MIC_{50}	MIC_{90}		Range	MIC_{50}	MIC_{90}		
Penicillin	≤ 0.03->8	2	>8	55	2->8	>8	>8	100	<0.001
Oxacillin	≤ 0.25	≤ 0.25	≤ 0.25	0	2->2	>2	>2	100	<0.001
Ampicillin	≤ 0.12->8	0.25	2	0	2->8	>8	>8	100	<0.001
Cefazolin	≤ 8	≤ 8	≤ 8	0	<4->16	≤ 8	>16	100	<0.001
Imipenem	≤ 1	≤ 1	≤ 1	0	≤ 1->8	8	>8	100	<0.001
Gentamicin	≤ 1->8	≤ 1	>8	31	≤ 1->8	>8	>8	66	<0.01
Erythromycin	≤ 0.25->4	≤ 0.25	>4	21	≤ 0.25->4	>4	>4	62	<0.001
Clindamycin	≤ 0.5-2	≤ 0.5	≤ 0.5	0	≤ 0.25->2	≤ 0.5	>2	36	<0.001
Minocycline	≤ 2	≤ 2	≤ 2	0	<1->8	≤ 2	≤ 2	4	0.278
Levofloxacin	≤ 0.5->4	≤ 0.5	4	24	≤ 0.5->4	4	>4	79	<0.001
Vancomycin	≤ 0.5-2	1	2	0	1-2	2	2	0	ND
ST	≤ 1->2	≤ 1	2	7	≤ 1->2	≤ 1	>2	26	<0.05

ST, sulfamethoxazole-trimethoprim. R, resistant. ND, not determined.

%R categorical variables were evaluated by the Chi-square test.

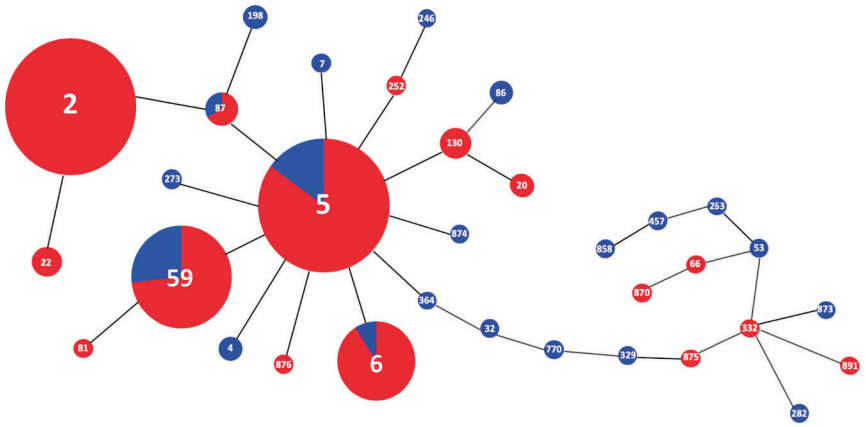

Figure 1 Minimum spanning tree based on the allelic profiles of 33 STs identified in 105 *S. epidermidis* isolates. Node sizes are proportional to the number of isolates for each ST and the numbers on connecting lines indicate the number of locus variants determined by pair-wise comparison. Red and blue areas represent MRSE and MSSE isolates, respectively.

in MSSE. No vancomycin resistance was detected in any isolate.

The 105 isolates were classified into 33 STs, including six newly assigned STs (ST870, ST873, ST874, ST875, ST876, and ST891) (**Figure 1**). Twenty-nine MSSE isolates were more diverse and were classified into 21 STs while the 76 MRSE isolates were classified into 16 STs. ST5 (n = 21, 20%) was the most prevalent of 33 STs, followed by ST2 (n = 19, 18%), ST59 (n = 15, 14%) and ST6 (n = 11, 10%). Among these four STs, MRSE isolates accounted for the largest proportion (100% for ST2, 86% for ST5, 91% for ST59, and 73% for ST6).

Table 2 Biocide susceptibility profiles of 105 *S. epidermidis* isolates

Biocides	MIC (μg/mL)				p-value
	Range	MIC_{50}	MIC_{90}	GM	
chlorhexidine					
MSSE (n=29)	≤ 0.5-2	1	2	1.05	0.001
MRSE (n=76)	≤ 0.25-4	1	2	1.44	
benzalkonium chloride					
MSSE (n=29)	≤ 0.5-8	2	8	2.48	0.004
MRSE (n=76)	≤ 1-8	4	8	4.30	
olanexidine gluconate					
MSSE (n=29)	≤ 0.5-2	2	2	1.40	<0.001
MRSE (n=76)	≤ 1-4	2	4	2.11	

GM, geometric mean of MICs. GMs were compared using the Mann-Whitney U-test.

Table 3 Prevalence of biocide resistance and biofilm development/adhesion-associated genes of 105 *S. epidermidis* isolates

	No. (%) of isolates		p-value
	MSSE	MRSE	
Biocide resistance genes			
qacA/B	3 (10.3)	39 (51.3)	<0.01
smr	12 (41.4)	33 (43.4)	0.85
Biofilm development/adhesion-associated genes			
sesI	1 (3.4)	12 (15.8)	0.086
icaA	7 (24.1)	25 (32.9)	0.38
bhp	10 (34.5)	24 (31.6)	0.78
aap	10 (34.5)	48 (63.2)	<0.01
atlE	29 (100)	76 (100)	ND
arcA	13 (44.8)	25 (32.9)	0.26
IS*256*	7 (24.1)	42 (55.3)	<0.01

ND, not determined. Categorical variables were evaluated by the Chi-square test.

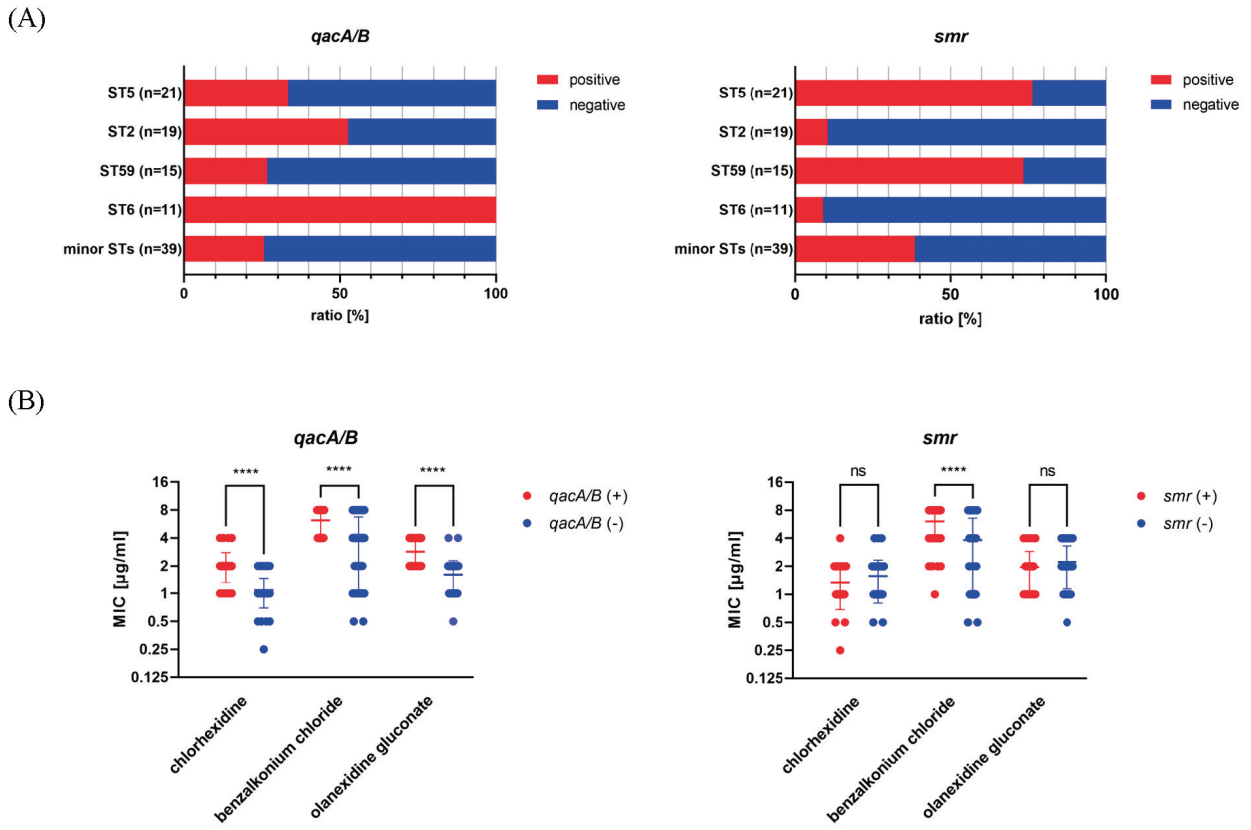

Figure 2 Prevalence of multidrug efflux pump-encoding genes and their association with biocide tolerance in 105 *S. epidermidis* isolates. (**A**) Prevalence of *qacA/B* and *smr* among each ST, and (**B**) the relationship between the presence of *qacA/B* and *smr* and three biocide MICs. Geometric means of biocide MICs were compared using the Mann-Whitney U-test. ****$p < 0.0001$.

B. Biocide MIC profiles and their association with STs and biocide tolerance genes

We investigated the relationship between the biocide MICs and STs. The geometric mean MICs of chlorhexidine, benzalkonium chloride, and olanexidine gluconate in the MRSE isolates were significantly higher than those in the MSSE isolates (**Table 2**). The prevalence of *qacA/B* was higher among the MRSE isolates (n = 39, 51%) than among the MSSE isolates (n = 3, 10%), whereas the prevalence of *smr* was similar between the MRSE and MSSE isolates (**Table 3**). ST6 and ST2 showed higher *qacA/B* positive rates of 100% and 53%, respectively, whereas the lowest frequencies of *smr* were observed in these two STs (9% and 11%, respectively) (**Figure 2A**).

The correlation between biocidal MICs and tolerance genes revealed that *qacA/B*-positive isolates showed significantly higher MICs for the three biocides than *qacA/B*-negative isolates (**Figure 2B**). However, *smr*-positive isolates exhibited significantly higher MIC for benzalkonium chloride.

C. SCC*mec* analysis and its association with STs

Our 76 MRSE isolates were classified into 15 different types of SCC*mec* including non-typeable types. Among the SCC*mec* elements detected and classified, SCC*mec* Type Ⅳ (2B) (n = 29, 38%) was predominant, followed by Type Ⅳ (2B & 5) (n = 11, 14%) (**Table 4**). However, 10 out of 15 different SCC*mec* types were classified as non-typeable SCC*mec* due to an unclassified combination of *mec* class and *ccr* type, and comprised 31 MRSE isolates (41%). Moreover, in terms of SCC*mec* types among the four major STs, the SCC*mec* types of ST6 isolates tended to be less diverse than those of the ST2, ST5, and ST59 isolates (**Table 4**).

D. Prevalence of biofilm development or adherence-associated genes

Next, we evaluated the frequency of virulence-associated genes, as *S. epidermidis* possesses several factors that are responsible for adhesion to host cells and biofilm formation. Among the MRSE strains, the frequency of *aap*, which is related to biofilm development through accumulation on polymer surfaces, and IS*256*, which is involved in biofilm production through the inactivation of *ica* operon-mediated phase variation by its insertion into *S. epidermidis*, was significantly higher than that of MSSE (**Table 3**). However, there was no significant difference in the prevalence of the other five genes between MRSE and MSSE.

sesI, which functions in cell-to-cell adhesion through the synthesis of a polysaccharide intercellular adhesin, and *icaA*, which is composed of the *ica* operon, were found in ST2 isolates (58% and 100%, respectively) (**Figure 3**). All ST2 strains were negative for *bhp*, a cell-wall anchored protein, whereas higher frequencies were found in ST5 and ST59 (52% and 67%, respectively). There were higher frequencies of *aap* among the three major strains, ST5, ST2, and ST59, whereas the prevalence of *arcA*, which encodes an arginine catabolic mobile element responsible for facilitating staphylococcal colonization of

Table 4 SCC*mec* profiles and its association with STs

SCC*mec*	*ccr*	*mec*	total MRSE (n=76)	Sequence type				
				ST2 (n=19)	ST5 (n=18)	ST59 (n=11)	ST6 (n=10)	other STs (n=18)
Type II	2	A	2	0	1	0	0	1
Type III	3	A	3	3	0	0	0	0
Type Ⅳ (2B)	2	B	29	1	4	8	9	7
Type Ⅳ (2B&5)	2, 5	B	11	4	3	1	0	3
Type XIV (5A)	5	A	1	1	0	0	0	0
Non-typeable 1	5	B	1	1	0	0	0	0
Non-typeable 2	2, 4	B	1	0	0	1	0	0
Non-typeable 3	2, 5	C	4	0	0	0	0	4
Non-typeable 4	3, 5	A	8	7	1	0	0	0
Non-typeable 5	4, 5	C	2	0	1	0	0	1
Non-typeable 6	2, 3, 5	A	1	1	0	0	0	0
Non-typeable 7	2	ND	7	0	7	0	0	0
Non-typeable 8	2, 5	ND	1	0	1	0	0	0
Non-typeable 9	ND	A	3	1	0	0	0	2
Non-typeable 10	ND	B	2	0	0	1	1	0

ND, not detected.

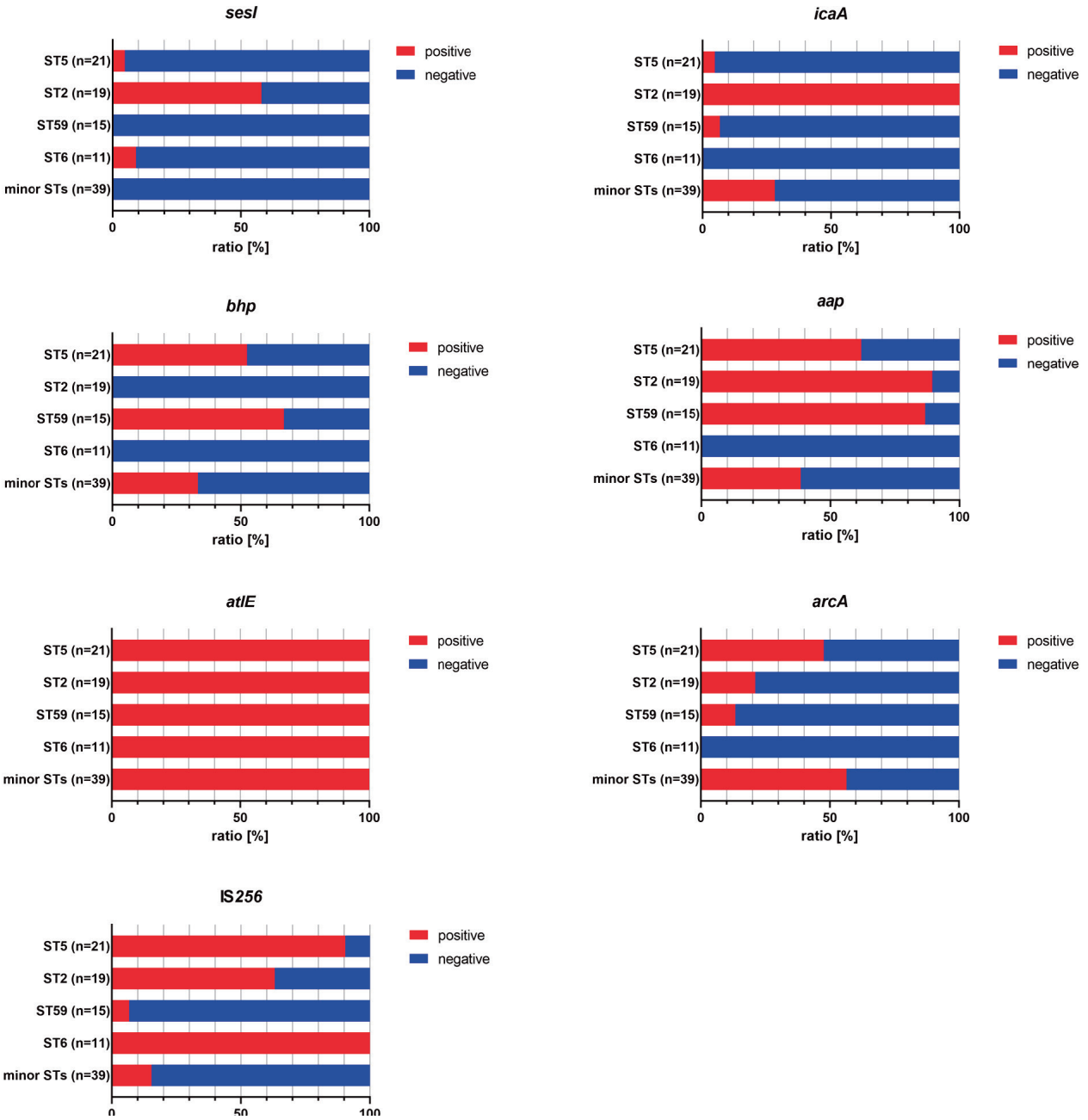

Figure 3 Prevalence of major biofilm development- or adhesion-associated genes among each ST. *sesI*, *icaA, bhp*, *aap, atlE*, *arcA*, and IS*256* identified in *Staphylococcu*s species were screened in 105 *S. epidermidis* isolates, as described in section C of Methods.

the skin and mucous membranes, was higher in the minor STs than in the three major STs. *atlE*, which mediates attachment to the polystyrene surface, was present in all isolates. Interestingly, ST6 was 100% positivity for IS*256* and 100% negativity for *icaA*, *aap*, *bhp*, and *arcA*.

E. Biofilm development ability

We further characterized the biofilm phenotypes of the 105 *S. epidermidis* isolates. Although the prevalence of strong producers in MRSE strains tended to be higher than that in MSSE, the total ratio of isolates with weak to strong biofilm formation was not significantly different between MRSE and MSSE ($p > 0.05$, **Figure 4A**).

Strong producers were concentrated in ST2 isolates among the four predominant ST groups but were also found in other STs (**Figure 4B**). Interestingly, all ST6 and many ST59 isolates were categorized as non-biofilm producers, indicating that there were different distributions of biofilm phenotypes among each ST.

IV. Discussion

S. epidermidis clinical isolates tend to be multidrug-resistant, with oxacillin resistant-MRSE ranging from

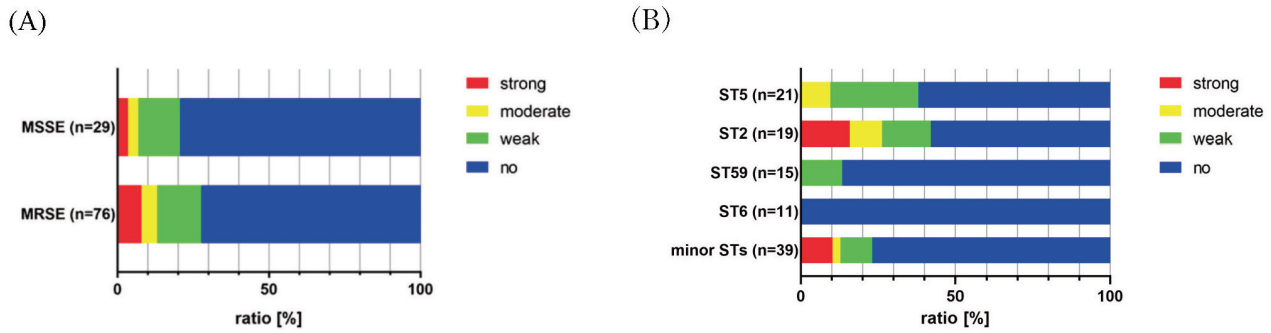

Figure 4 Biofilm development ability of 105 *S. epidermidis* isolates. (**A**) Prevalence of each biofilm phenotype in MSSE and MRSE isolates, and (**B**) relationship between the biofilm phenotype and STs. The phenotype was categorized, as described in section D of Methods.

70–90% prevalence, including data from nationwide surveillance in Japan[1)3)24)]. Our results agree with this, highlighting that MSSE remains highly susceptible to several antimicrobials and that vancomycin is still recommended for treating MRSE infections. Our findings support the need to monitor antimicrobial resistance to effectively treat *S. epidermidis* infections.

S. epidermidis, especially MRSE, is a major reservoir of antimicrobial and biocidal resistance determinants[4)]. In this study, MRSE isolates possessed higher rates of *qacA/B* than MSSE isolates and were associated with a higher tolerance to three low-level antiseptics. These results, coupled with those of previous studies on *Staphylococcus* species[2)25)], demonstrate that antimicrobial and antiseptic co-resistant/tolerant isolates may be spreading in Japanese hospitals. However, as QacA/B and Smr cannot functionally exhaust many intermediate-level antiseptics/disinfectants that are often used in healthcare facilities, such as ethanol[26)], from inside bacterial cells, appropriate antiseptics/disinfectants may be efficient in eliminating antiseptic/disinfectant-tolerant isolates.

Methicillin-resistant CoNS, including *S. epidermidis*, possesses multiple SCC*mec* elements, resulting in diverse structural variants[19)27)]. Consistent with previous reports[19)27)], our results demonstrated that diverse SCC*mec* elements, including SCC*mec* type IV, were predominant, suggesting that CoNS in Japan may constitute a reservoir of SCC*mec* with methicillin resistance. Moreover, a previous study reported that SCC*mec* islands could evolve through site-specific recombination at this locus during adaptation to the human host[28)]. Therefore, we may need to characterize SCC*mec* islands at the whole-genome level to clarify the global diversification of *S. epidermidis* used in this study.

We demonstrated that MRSE isolates frequently possessed the biofilm-forming or adherence-associated genes *aap* and IS*256*; these higher rates did not result in significant differences in phenotypic biofilm formation between MRSE and MSSE. This may be because major biofilm development- or adhesion-associated genes were not fully upregulated in the planktonic cells used in this study or because other determinants regulating the biofilm production process were present in our isolates. However, coupled with the results of antimicrobial/antiseptic co-resistance/tolerance, our findings suggest that highly pathogenic multidrug-resistant *S. epidermidis* isolates have already been disseminated in Japan. In addition, a previous study from China demonstrated that ST2 isolates were exclusively *ica*- and IS*256*-positive and biofilm-forming[6)]. Our results showed a similar tendency, indicating for the first time that ST2 MRSE isolates might have higher pathogenicity among the four major STs in our isolates. Extracellular biofilms inhibit the action of most antimicrobials, thereby impairing the treatment of *Staphylococcus* medical-device infections. This indicates that the consistent application of infection prevention measures at an appropriate point, such as the periprocedural period, is crucial, in concordance with previous studies[2)13)]. Moreover, previous studies have demonstrated that exopolysaccharides, such as polysaccharide intercellular adhesins, protect *S. epidermidis* from host defense mechanisms such as neutrophil killing[1)29)]. Therefore, further investigation is needed to elucidate the relationship between STs, prevalence of virulence factors, and pathogenicity.

Among global high-risk *S. epidermidis* clones, ST2 belongs to the CC2 strain, which is the most widespread healthcare-associated strain[2)5)6)]. However, there are limited reports focusing on the genetic features of ST2 MRSE, none of which are from Japan. The results of our MLST analysis provide novel insights that multidrug-resistant *S. epidermidis* CC2 isolates, including ST2 and ST5, may already be predominant and have adapted to healthcare facility environments in Japan. Further de-

tailed genetic analysis using whole-genome sequencing may contribute to the understanding of genetic diversity and features that remain unidentified in antimicrobial resistance, virulence, and pathogenicity in CC2 MRSE healthcare-associated strains in Japan.

The current study had some limitations. For example, the number of clinical isolates collected from the two hospitals was small, and they were not compared with the isolates from healthy participants, and detailed information such as the isolated numbers and wards of this organism involved in horizontal transmission in each hospital was not investigated.

V. Conclusion

Highly virulent, multidrug-resistant *S. epidermidis* isolates have emerged in Japan, complicating infection prevention and treatment. Our findings provide novel insights and reveal that the global ST2 MRSE clone and its close genetic lineages may have already been disseminated and have persisted for a long time in Japanese healthcare facilities. Therefore, robust surveillance systems and infection control and prevention measures based on continuous monitoring of their lineages are crucial for their elimination.

Acknowledgement

This study was supported by the Japanese Society of Laboratory Medicine Fund for the Promotion of Scientific Research. We would like to thank Editage (www.editage.jp) for English language editing.

Disclosures

We declare that we have no conflicts of interest. All authors read and approved the final manuscript.

References

1) Otto M. *Staphylococcus epidermidis*--the 'accidental' pathogen. Nat Rev Microbiol 2009; 7 (8) : 555-67.
2) Månsson E, Bech Johannesen T, Nilsdotter-Augustinsson Å, et al. Comparative genomics of *Staphylococcus epidermidis* from prosthetic-joint infections and nares highlights genetic traits associated with antimicrobial resistance, not virulence. Microb Genom 2021; 7 (2) .
3) Japan Nosocomial Infections Surveillance Ministry of Health, Labour and Welfare, https://janis.mhlw.go.jp/english/report/index.html, (assessed Dec 20, 2022) .
4) Otto M. Coagulase-negative staphylococci as reservoirs of genes facilitating MRSA infection: Staphylococcal commensal species such as *Staphylococcus epidermidis* are being recognized as important sources of genes promoting MRSA colonization and virulence. Bioessays 2013; 35 (1) : 4-11.
5) Lee JYH, Monk IR, Gonçalves da Silva A, et al. Global spread of three multidrug-resistant lineages of *Staphylococcus epidermidis*. Nat Microbiol 2018; 3 (10) : 1175-85.
6) Li M, Wang X, Gao Q, et al. Molecular characterization of *Staphylococcus epidermidis* strains isolated from a teaching hospital in Shanghai, China. J Med Microbiol 2009; 58 (Pt 4) : 456-61.
7) Miragaia M, Thomas JC, Couto I, et al. Inferring a population structure for *Staphylococcus epidermidis* from multilocus sequence typing data. J Bacteriol 2007; 189 (6) : 2540-52.
8) Clinical and Laboratory Standards Institute. Performance Standards for Antimicrobial Susceptibility Testing: 30th Edition M100-ED30. CLSI, Wayne, PA, USA, 2020.
9) Pérez-Roth E, Claverie-Martín F, Villar J, et al. Multiplex PCR for simultaneous identification of *Staphylococcus aureus* and detection of methicillin and mupirocin resistance. J Clin Microbiol 2001; 39 (11) : 4037-41.
10) Bowden MG, Chen W, Singvall J, et al. Identification and preliminary characterization of cell-wall-anchored proteins of *Staphylococcus epidermidis*. Microbiology (Reading) . 2005; 151 (Pt 5) : 1453-64.
11) Najar Peerayeh S, Jazayeri Moghadas A, Behmanesh M. Prevalence of Virulence-Related Determinants in Clinical Isolates of *Staphylococcus epidermidis*. Jundishapur J Microbiol 2016; 9 (8) : e30593.
12) Møretrø T, Hermansen L, Holck AL, et al. Biofilm formation and the presence of the intercellular adhesion locus *ica* among staphylococci from food and food processing environments. Appl Environ Microbiol 2003; 69 (9) : 5648-55.
13) Du X, Zhu Y, Song Y, et al. Molecular analysis of *Staphylococcus epidermidis* strains isolated from community and hospital environments in China. PLoS One 2013; 8 (5) : e62742.
14) Gu J, Li H, Li M, et al. Bacterial insertion sequence IS*256* as a potential molecular marker to discriminate invasive strains from commensal strains of *Staphylococcus epidermidis*. J Hosp Infect 2005; 61 (4) : 342-8.
15) Ho CM, Li CY, Ho MW, et al. High rate of *qacA*- and *qacB*-positive methicillin-resistant *Staphylococcus aureus* isolates from chlorhexidine-impregnated catheter-related bloodstream infections. Antimicrob Agents Chemother 2012; 56 (11) : 5693-7.
16) Thomas JC, Vargas MR, Miragaia M, et al. Improved multilocus sequence typing scheme for *Staphylococcus epidermidis*. J Clin Microbiol 2007; 45 (2) : 616-9.
17) Nascimento M, Sousa A, Ramirez M, et al. PHYLOViZ 2.0: providing scalable data integration and visualization for multiple phylogenetic inference methods. Bioinformatics 2017; 33 (1) : 128-9.
18) Kondo Y, Ito T, Ma XX, et al. Combination of multiplex PCRs

for staphylococcal cassette chromosome *mec* type assignment: rapid identification system for *mec*, *ccr*, and major differences in junkyard regions. Antimicrob Agents Chemother 2007; 51(1): 264-74.

19) Ruppé E, Barbier F, Mesli Y, et al. Diversity of staphylococcal cassette chromosome *mec* structures in methicillin-resistant *Staphylococcus epidermidis* and *Staphylococcus haemolyticus* strains among outpatients from four countries. Antimicrob Agents Chemother 2009; 53(2): 442-9.

20) Classification of staphylococcal cassette chromosome *mec* (SCC*mec*): guidelines for reporting novel SCC*mec* elements. Antimicrob Agents Chemother 2009; 53(12):4961-7.

21) Christensen GD, Simpson WA, Younger JJ, et al. Adherence of coagulase-negative staphylococci to plastic tissue culture plates: a quantitative model for the adherence of staphylococci to medical devices. J Clin Microbiol 1985; 22(6): 996-1006.

22) O'Neill E, Pozzi C, Houston P, et al. A novel *Staphylococcus aureus* biofilm phenotype mediated by the fibronectin-binding proteins, FnBPA and FnBPB. J Bacteriol 2008; 190(11): 3835-50.

23) Asante J, Hetsa BA, Amoako DG, et al. Genomic Analysis of Antibiotic-Resistant *Staphylococcus epidermidis* Isolates From Clinical Sources in the Kwazulu-Natal Province, South Africa. Front Microbiol 2021; 12: 656306.

24) Henriksen AS, Smart J, Hamed K. Comparative activity of ceftobiprole against coagulase-negative staphylococci from the BSAC Bacteraemia Surveillance Programme, 2013-2015. Eur J Clin Microbiol Infect Dis 2018; 37(9): 1653-9.

25) Kim H, Park S, Seo H, et al. Clinical impact of and microbiological risk factors for *qacA/B* positivity in ICU-acquired ST5-methicillin-resistant SCC*mec* type II *Staphylococcus aureus* bacteremia. Sci Rep 2022; 12(1): 11413.

26) McDonnell G, Russell AD. Antiseptics and disinfectants: Activity, action, and resistance. Clinical Microbiology Reviews 1999; 12(1): 147-79.

27) Hanssen AM, Sollid JU. Multiple staphylococcal cassette chromosomes and allelic variants of cassette chromosome recombinases in *Staphylococcus aureus* and coagulase-negative staphylococci from Norway. Antimicrob Agents Chemother 2007; 51(5): 1671-7.

28) Datta MS, Yelin I, Hochwald O, et al. Rapid methicillin resistance diversification in *Staphylococcus epidermidis* colonizing human neonates. Nat Commun 2021; 12(1): 6062.

29) Rautenberg M, Joo HS, Otto M, et al. Neutrophil responses to staphylococcal pathogens and commensals *via* the formyl peptide receptor 2 relates to phenol-soluble modulin release and virulence. FASEB J 2011; 25(4): 1254-63.

Original

Verification of individual differences in visual judgment of urine test strips and proposal of objective evaluation method

*†Keigo Inagaki*1, Katsumasa Nakamura*2*

†Correspondence: Cooperative Major in Medical Photonics, Hamamatsu University School of Medicine, Shizuoka, Japan.
Institute for Medical Photonics Research, Hamamatsu University School of Medicine, 1-20-1 Handayama, Higashi-ku, Hamamatsu City, Shizuoka, Japan.
E-mail: kinagaki@hama-med.ac.jp
Received August 10, 2023; accepted March 25, 2024
*1 Institute for Medical Photonics Research, Hamamatsu University School of Medicine, Shizuoka, Japan
*2 Faculty of Medicine, Hamamatsu University School of Medicine, Shizuoka, Japan

ABSTRACT

Objective: Practitioners at small-scale medical check-up facilities lacking automatic urine analyzers visually analyze and interpret urine test strips. However, visual judgment is liable to human errors in estimating parameters and variations in judgment time. Therefore, to objectively judge the color of urine test strips, we developed an automated urine test strip colorimetric program using images taken with a smartphone camera.
Materials and Methods: For urinalysis, 40 urine samples were randomly selected, and six nurses were included as evaluators. The effectiveness of the program was confirmed by determining the differences in visual judgment among evaluators. A color chart was used as a judgment reference table for the comparison of visual judgment of urinalysis test strips. Two automatic urine analyzers, US-3500 (Eiken Chemical Co., Ltd.) and LABOSPECT 006 (Hitachi High-Tech Co., Ltd.), were used for the comparative evaluation.
Results: The study showed slight inter-rater differences in the evaluation of most parameters, including protein, glucose, ketone, specific gravity, occult blood, leukocytes, and nitrite; however, individual differences were observed for urobilinogen, bilirubin, pH, creatinine, and albumin. Moreover, we compared visual judgment to the new program and observed that the agreement rate of the automated urine test strip colorimetric program (81.9%) was higher than that of visual judgment (75.1%).
Conclusion: Based on our findings, we propose an inexpensive and simple method for the stable evaluation of urine test strips for urinalysis that is unaffected by human error during visual judgment.

〔Lab Med Int 2024; 3(2): 42-49〕

Key Words
urine test strip, visual judgment, objective evaluation, colorimetry

I. Introduction

Urinalysis is one of the most frequently performed tests in healthcare settings; it is inexpensive and used to detect risk signals for key metabolic functions using urine samples [1]. Test papers are used in a simple urine test. Because this method is inexpensive and non-invasive, it has been widely used as an effective tool for diagnosing several diseases, including urinary tract infections, renal disorders, cardiovascular diseases, and metabolic dysfunctions, such as diabetes and liver diseases [2) 3)]. In general hospitals, automatic urine analyzers are introduced to evaluate urine test strips, thereby avoiding human errors that may arise due to the systemization of examination rooms, especially in such large facilities. However, introducing an expensive automatic urine analyzer is not feasible for general practitioners at small-scale examination facilities. Therefore, visual judgment

is performed in such facilities. However, the judgment time of each parameter differs in urinalysis using test strips, and determining all parameters within the set time is difficult. In addition, color evaluation is affected by environmental factors, such as the color and intensity of illumination during observation, making accurate determination challenging. In a previous study, Winkens et al. observed a lack of agreement between interobserver and intraobserver urinalysis results using multiple test strips [4]. In contrast, Bekhof et al. reported that interobserver agreement was highly effective, and the interobserver scores of urinalysis test strips did not deviate for multiple categories [5]. In addition, a previous study in Japan reported that the subjective judgments of nurses resulted in differences in color expression and opinions [6]. Determining the color of the test strip for urinalysis provides important information regarding the early detection of abnormalities; therefore, performing an accurate evaluation is necessary. In particular, inexperienced nurses may find it difficult to accurately judge and communicate color information [7]. In addition, the number of male nurses has increased in recent years, and 1 in 20 men have congenital color blindness [8].

Numerous previous reports have focused on the objective evaluation of urinalysis test strips using smartphones [9)–11)]. Studies on judgments by machine learning based on hue have been performed thus far, but few have focused on color differences in judging urinalysis test strips. If the strips can be judged solely based on color difference, machine learning may not be required. In addition, regardless of the manufacturer of the test paper, the standard color chart data for urinalysis test papers can be used for evaluation. In addition to smartphones, urine test strips have been evaluated using scanners [12], and ongoing research is investigating methods that can be consistently and universally used by all practitioners. However, to date, only a few, inadequate validated studies exist on the simultaneous evaluation of interindividual visual assessment differences and program effectiveness using urine specimens from patients. In addition, there is no consensus regarding the presence or absence of individual differences in visual judgment.

The present study aimed to address these issues by developing an automated urine test strip colorimetric program for automatic analysis of urine test strips from images taken with a smartphone [13]. This study included six nurses to investigate the individual differences in visual judgment of urinalysis test strips. Using the results of an automatic urine analyzer as the gold standard, we investigated the rate of agreement between the visual judgment of urine test strips and the automatic urine test strip colorimetric program.

II. Materials and methods

Figure 1 demonstrates the experimental protocol used in this study. A photography box (PU5025B: PULUZ) was used to provide constant lighting. The smartphone used was the Xperia 5II (XQ-AS42: SONY) equipped with the standard lens of a triple-lens camera (ZEISS lens). Other parameters were as follows: sensor size, 1/1.7-inch large format; number of effective pixels, approximately 12.2 million; focal length, 24 mm; F value, 1.7; dual photodiode; and hybrid image stabilization (optical + electronic). The urinalysis test strip (Uropaper® III 'Eiken' (E-UR97): Eiken Chemical Co. Ltd.) used was capable of testing 12 parameters. The color chart shown in **Figure 1**, which is commonly used in clinical practice, was used as a judgment reference table for comparison of visual judgment of urinalysis test strips. For urinalysis, 40 samples were randomly selected from the laboratory

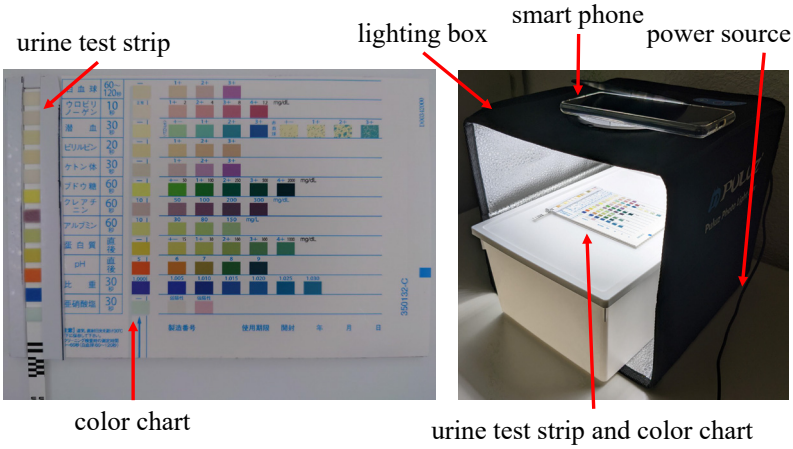

Figure 1 Experiment apparatus

departments of hospitals in H city. Basic information on the specimens is provided in **Table 1**. Two automatic urine analyzers, US-3500 (Eiken Chemical Co., Ltd.) and LABOSPECT 006 (Hitachi High-Tech Co., Ltd.), were used for comparative evaluation. US-3500 was used to compare urobilinogen, occult blood, protein, glucose, ketone bodies, bilirubin, nitrite, specific gravity, white blood cells, and pH. LABOSPECT 006 was used to compare creatine and albumin levels.

Table 1 Basic information on urine specimens

Contents	Number of people (%)
Sex	
Female	21 (52.5)
Male	19 (47.5)
Average age, years	
Female	45.86 ± 18.2
Male	66.89 ± 15.7
Clinical department	
General surgery	1 (2.5)
Lower gastrointestinal surgery	1 (2.5)
Liver internal medicine	1 (2.5)
Ophthalmology	1 (2.5)
Hematology	1 (2.5)
Vascular surgery	1 (2.5)
Obstetrics and gynecology	8 (20.0)
Cardiology	1 (2.5)
Pediatrics	1 (2.5)
Upper gastrointestinal surgery	3 (7.5)
Nephrology	3 (7.5)
Orthopedics	5 (12.5)
Endocrine	2 (5.0)
Urology	10 (25.0)
Immunology	1 (2.5)

We acquired data on urobilinogen, occult blood, protein, glucose, ketone bodies, bilirubin, nitrite, specific gravity, white blood cells, and pH for all 40 samples using automatic analyzers. However, we could only obtain data on creatine levels from five samples and albumin from one sample using automatic analyzers. The automatic urine test strip colorimetric program developed in this study was created on a desktop computer (HP EliteDesk 800 G4 TWR: HP). The development language was Python, and the OpenCV library was used for image processing.

Experimental methods

Visual judgment

Visual judgment was performed by six individuals (four male and two female individuals) who had no eye disease and had nursing qualifications. During the visual judgment of samples, the individuals were adequately spaced to prevent any potential interference with each other's results. The specific procedure followed during judgment is detailed below:

(1) Turn on the shooting box (leave for 30 min for light stabilization).
(2) Enter the patient ID on the entry form.
(3) Start the survey after 30 min of turning on the power.
(4) Soak urinalysis test strips completely in urine samples for approximately 1–2 s.
(5) Gently tap the side of the test paper onto a tissue paper to remove excess urine.
(6) Place the color chart and test paper into the photography box.
(7) Within 30–60 s of soaking the sample in urine and removing it from the spitz, determine the closest color

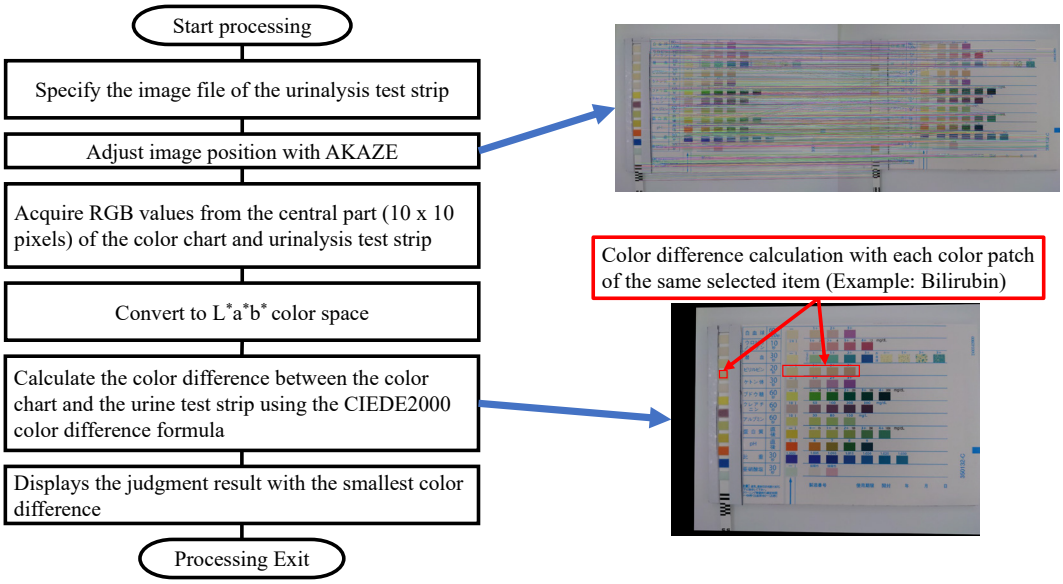

Figure 2 Processing flow

on the color chart and check it on the entry form for visual judgment.

(8) Repeat steps (4) to (7) for all samples.

Judgment by an automated urine test strip colorimetric program

・Automated urine test strip colorimetric program

Figure 2 demonstrates the process flow of an automated urine test strip colorimetric program. The colors of the urinalysis test papers and those of the color chart were compared as per the following procedure, and each parameter was judged accordingly.

(1) Specify the image file of the urinalysis test strip.

(2) Adjust the position of the image with AKAZE.

(3) Acquire RGB values from the central part (10 × 10 pixels) of the color chart and urinalysis test strip.

(4) Convert to L*a*b* color space.

(5) Calculate the color difference between the color chart and urine test strip using the CIEDE2000 color difference formula (color difference calculation with each color patch of the same selected item).

(6) Record the judgment result with the smallest color difference.

・Filming environment and procedures

Similar to visual evaluation, color evaluation was performed using the photography box (PU5025B: PULUZ) under the same environment.

(1) Turn on the shooting box (leave for 30 min for light stabilization).

(2) Start shooting after 30 min of turning on the power.

(3) Install the smartphone with an activated camera on the top of the shooting box (set the color temperature of the camera to sunlight, which is the same as the color temperature of lighting inside the shooting box).

(4) Soak urine test strips completely in urine for approximately 1–2 s.

(5) Gently tap the side of the test paper onto a tissue paper to remove excess urine.

(6) Place the test paper in the shooting box.

(7) Take a picture of the sample 50 s after removing it from the spitz.

(8) Judge the photographed images using the automatic urine dipstick colorimetric program.

(9) Obtain data regarding age, sex, clinical department, urinalysis results, and oral medication status (presence or absence of sodium-glucose co-transporter 2 inhibitors) from electronic medical records.

(10) Confirm whether the results match those obtained from the automatic urine analyzer.

Statistical analysis

The target sample size for intraclass correlation coefficient (ICC) (2.1) was set at 40 with reference to a study by Doros et al[14]. (assuming six examiners, an ICC of 0.8, a significance level of 0.05, and a confidence interval of 0.2, the required number of cases is 32). ICC (2.1) was used for inter-rater reliability. The statistical software IBM SPSS Statistics 25.0 (IBM Corp., Armonk, NY, USA) was used for ICC calculations. The rate of agreement was calculated as the rate of agreement with the results obtained from the automatic urine analyzer (number of matched urine specimens/number of specimens investigated).

Ethical considerations

This research was reviewed and approved by the ethics committee of Hamamatsu University School of Medicine (approval number: 21-239).

III. Results

Table 2 lists the ICC (2.1) for each parameter of urinalysis using test strips. The reference ICC criteria reported by Landis et al. were used[15]. Glucose, occult blood, leukocytes, and nitrite were within the Almost Perfect criteria. Protein, ketone, specific gravity, and albumin were within the Substantial criteria. Urobilinogen, pH, and creatinine were within the Moderate criteria. Bilirubin was within the Fair criteria. Cronbach's alpha was 0.8 or higher for all parameters.

Table 3 shows the comparison of the results of the automatic urine analyzer, visual judgment, and automated urine test strip colorimetric program. The values in the table indicate the concordance rate of judgment results with that of the automatic urine analyzer; A–F show the results of visual judgment by the six examiners, examin-

Table 2 Intraclass correlation coefficient of inter-examiner reliability

Parameter	ICC (2.1) (95% CI)	Cronbach's alpha	p-value
Protein	0.783 (0.690–0.863)	0.959	<0.001
Glucose	0.941 (0.909–0.965)	0.990	<0.001
Urobilinogen	0.422 (0.289–0.575)	0.821	<0.001
Bilirubin	0.377 (0.246–0.533)	0.801	<0.001
Ketone	0.794 (0.705–0.870)	0.958	<0.001
Specific gravity	0.742 (0.616–0.842)	0.958	<0.001
Occult blood	0.864 (0.799–0.916)	0.976	<0.001
pH	0.529 (0.347–0.692)	0.916	<0.001
Leukocytes	0.883 (0.825–0.928)	0.979	<0.001
Nitrite	0.907 (0.860–0.943)	0.983	<0.001
Creatinine	0.516 (0.349–0.675)	0.904	<0.001
Albumin	0.661 (0.538–0.776)	0.930	<0.001

ICC, intraclass correlation coefficient; CI, confidence interval

er avg. indicates the average of the A–F results, and the program indicates the results from the automatic urine test strip colorimetric program. Urobilinogen, occult blood, protein, glucose, ketone bodies, bilirubin, nitrite, specific gravity, leukocytes, and pH were evaluated for concordance across 40 samples (N = 40). Data for creatinine and albumin could not be obtained from the automated urine analyzer due to the small number of test requests per day. Therefore, the concordance rate was evaluated using data obtained for five specimens (N = 5) of creatine and one specimen (N = 1) of albumin from the automatic urine analyzer.

A comparison of the results of the average visual judgment (Examiner avg.) and the automated urine test strip colorimetric program (Program) revealed that the agreement rate of judgment by the colorimetric program was high. Moreover, the average match rate of all 12 parameters was 75.1% for visual judgment and 81.9% for the automated urine test strip colorimetric program. Concordance was better using the automated urine test strip colorimetric program. The lowest agreement rate of judgment results of specific gravity was observed with the automated urine analyzer for both visual determination and the automated urine test strip colorimetric program.

Table 4 shows the agreement rate of ± 1 rank with the automatic urine analyzer. The average ± 1 rank agreement rate for the 12 items was 92.8% for the examiners and 92.9% for the program.

IV. Discussion

In the present study, we recruited six nurses to investigate individual differences in visual judgment of urinalysis test strips. Using the results from the automatic urine analyzer as the gold standard, we investigated the agreement rate between the results of visual judgment of urine

Table 3 Concordance rate with the automated urine analyzer

Parameter	A	B	C	D	E	F	Examiner avg.	Program
Protein	72.5	85.0	82.5	82.5	87.5	87.5	82.9	92.5
Glucose	97.5	97.5	95.0	100.0	90.0	97.5	96.3	95.0
Urobilinogen	82.5	92.5	77.5	95.0	90.0	90.0	87.9	92.5
Bilirubin	67.5	90.0	62.5	95.0	82.5	80.0	79.6	75.0
Ketone	95.0	97.5	87.5	97.5	92.5	95.0	94.2	100.0
Specific gravity	10.0	7.5	10.0	37.5	27.5	10.0	17.1	7.5
Occult blood	90.0	90.0	92.5	90.0	92.5	90.0	90.8	90.0
pH	67.5	82.5	70.0	35.0	52.5	62.5	61.7	82.5
Leukocytes	85.0	85.0	85.0	77.5	82.5	82.5	82.9	90.0
Nitrite	97.5	97.5	97.5	97.5	97.5	100.0	97.9	97.5
Creatinine	60.0	60.0	80.0	60.0	20.0	80.0	60.0	60.0
Albumin	100.0	100.0	0.0	0.0	0.0	100.0	50.0	100.0
Average of 12 parameters	77.1	82.1	70.0	72.3	67.9	81.3	75.1	81.9

Examiner avg., average visual judgment; Program, automated urine test strip colorimetric program

Table 4 The ± 1 rank agreement rate with the automatic urine analyzer

Parameter	A	B	C	D	E	F	Examiner avg.	Program
Protein	100.0	100.0	100.0	97.5	100.0	100.0	99.6	100.0
Glucose	100.0	100.0	100.0	100.0	97.5	100.0	99.6	100.0
Urobilinogen	100.0	100.0	100.0	100.0	100.0	100.0	100.0	100.0
Bilirubin	100.0	97.5	95.0	100.0	100.0	97.5	98.3	100.0
Ketone	100.0	100.0	97.5	100.0	100.0	100.0	99.6	100.0
Specific gravity	30.0	25.0	30.0	27.5	42.5	20.0	29.2	17.5
Occult blood	97.5	97.5	97.5	97.5	97.5	97.5	97.5	97.5
pH	97.5	100.0	97.5	65.0	97.5	100.0	92.9	100.0
Leukocytes	100.0	97.5	97.5	92.5	97.5	97.5	97.1	100.0
Nitrite	100.0	100.0	100.0	100.0	100.0	100.0	100.0	100.0
Creatinine	100.0	100.0	100.0	100.0	100.0	100.0	100.0	100.0
Albumin	100.0	100.0	100.0	100.0	100.0	100.0	100.0	100.0
Average of 12 parameters	93.8	93.1	92.9	90.0	94.4	92.7	92.8	92.9

test strips and the automatic urine test strip colorimetric program.

ICC (2.1) was calculated as the inter-examiner reliability of the six nurses to investigate individual differences in visual judgment of urinalysis test strips. As Cronbach's alpha was 0.8 or higher for all parameters, it was assumed that the internal consistency among raters is maintained; an ICC (2.1) value of 0.7 or higher generally indicates high reliability [16]. The parameters with an ICC (2.1) value of 0.7 or higher were protein, glucose, ketone, specific gravity, occult blood, leukocytes, and nitrite. Urobilinogen, bilirubin, pH, creatinine, and albumin had ICC (2.1) values less than 0.7. Although there were slight inter-rater differences for the parameters of protein, glucose, ketone, specific gravity, occult blood, leukocytes, and nitrite, differences were observed for urobilinogen, bilirubin, pH, creatinine, and albumin. These discrepancies may be attributed to the fact that the color changes caused by the application of urine may be different from the colors in the chart or may fall between adjacent colors. One of the evaluators recorded cases of difficult judgment when the color did not match any one of the color charts or fell between adjacent colors. In addition, the measurement time specified for urinalysis test strips was 30–60 s. As 12 parameters need to be judged within 30 s, it is difficult to judge similar colors, and there is a possibility of errors in judgment. In the future, it will be necessary to use instruments, such as a spectrophotometer or color difference meter, to measure the color difference between adjacent colors on the color chart, determine the color of urine test paper after adding urine, and verify the underlying cause for the color similarity.

In the present study, a comparison of the visual judgment and automated urine test strip colorimetric program revealed that the agreement rate of ± 1 rank for each item, other than specific gravity, for both the examiner and the program, was over 90%. Furthermore, the agreement rate between the average value of the results for all 12 items and the average value of visual judgment was 75.1%. For the automated urine test strip colorimetric program, the average concordance rate for all 12 parameters was 81.9%, indicating a higher concordance rate. Urobilinogen, bilirubin, pH, creatinine, and albumin, which showed an ICC (2.1) value of less than 0.7, had higher than the average agreement rates using the automated urine test strip colorimetric program for all parameters except bilirubin. Considering the rate of concordance for each evaluator in visual judgment, some parameters differ depending on the evaluator. Regarding specific gravity, the ICC (2.1) yielded good results within the range of substantial criteria, but the concordance rate was significantly low, ranging from 7.5% to 37.5%. All judges noted that none of the colors on the color chart matched for specific gravity. Therefore, the matching rate is low because no matching color is displayed on the color chart after staining with urine. In the future, objective evaluation of colors using a spectrophotometer or color difference meter will be necessary. In addition, creatine and albumin had ICC (2.1) values of 0.516 and 0.661, respectively, indicating low inter-examiner reliability. As a small number of data points were obtained from the automated urine analyzer, the concordance rate is only for reference, and this method is considered effective.

Although several studies have evaluated program reliability using artificial urine and reagents [17)–19)], only a few studies evaluating program reliability using actual urine specimens are available. Rahmat et al. validated scanner color comparison using real urine specimens and reported an accuracy of 95.45% using a high-resolution scanner [12]. A low-resolution scanner reported an accuracy of 83%, which is comparable to the results of the automated urine test strip colorimetric program in this study. In addition, Africa et al. verified the accuracy of color comparison using 45 samples from an accredited urinalysis laboratory and reported an accuracy of 96.51% [20]; in this study, classification was performed using not only color comparison but also machine learning, resulting in improved accuracy. Although the automated urine test strip colorimetric program developed in the present study does not require data for learning, it is less accurate than the program developed by Africa et al [20].

Imaging using smartphones to analyze urinalysis test strips may support point-of-care testing in home settings [18) 21)]. An FDA-approved product that uses a smartphone application to test the parameters of urinalysis test strips for early detection of chronic kidney disease and urinary tract infections is available in the market [22] (Healthy.io, https://healthy.io/), and smartphone applications, such as "Vivoo" [23] and "Uchek" [24], have been developed. Moreover, attention is being paid to the use of point-of-care tests for health management at home because people are refraining from medical examinations due to the coronavirus pandemic.

This study has several limitations. First, the sample size is limited to 40. Furthermore, as this method requires many items and the steps are complicated, it may lead to measurement errors depending on the technique of the individual performing the evaluation. Therefore, it is important to reduce the number of required items and simplify the procedure. Moreover, the current automated

urine test strip colorimetric program requires comparison with the standard color chart of each urine test strip manufacturer. Therefore, we are aiming to add a feature that will allow users to save the standard color charts from manufacturers that are mainly used in clinical practice and select the urine test strips to be used within the app. As part of the internal and external quality control surveys for the app, we intend to conduct multiple measurements of the same sample, having multiple people operate the program, and acquiring samples at multiple facilities.

V. Conclusion

The automatic urine test strip colorimetric program developed in the present study is a program that focuses only on color differences; therefore, it does not require a large amount of prior data for machine learning. In addition, if the standard color chart data of each manufacturer is available, processing urinalysis test strips produced by various manufacturers worldwide without the need for calibration is possible. However, because only 40 samples were analyzed in this study, concordance rates need to be verified in additional samples to determine the effectiveness of the automated urine test strip colorimetric program. Therefore, in the future, we plan to validate the automated urine test strip colorimetric program using a large number of urine specimens.

Conflicts of interest

The authors declare no conflict of interest.

Funding source

This study was supported by TERUMO LIFE SCIENCE FOUNDATION [grant number 21-III 7009] and the HUSM Grant-in-Aid for manuscript writing.

Acknowledgement

We would like to thank Takuya Kanamori, Ami Kinpara, Kouhei Sugiura, Toshinobu Moriyama, and Mitsue Tanaka for their cooperation in this research.

Authorship contributions

All authors were involved in the preparation of the manuscript and reviewed the final manuscript.

References

1) Prah JK, Amoah S, Ocansey DW, et al. Evaluation of urinalysis parameters and antimicrobial susceptibility of uropathogens among out-patients at University of Cape Coast Hospital. Ghana Med J 2019; 53(1): 44-51. doi: 10.4314/gmj.v53i1.7.
2) Simerville JA, Maxted WC, Pahira JJ. Urinalysis: A comprehensive review. Am Fam Phys 2005; 71(6): 1153-62.
3) Devillé WLJM, Yzermans JC, van Duijn NP, et al. The urine dipstick test useful to rule out infections. A meta-analysis of the accuracy. BMC Urol 2004; 4: 4. doi: 10.1186/1471-2490-4-4.
4) Winkens RA, Leffers P, Degenaar CP, et al. The reproducibility of urinalysis using multiple reagent test strips. Eur J Clin Chem Clin Biochem 1991; 29(12): 813-8. doi: 10.1515/cclm.1991.29.12.813.
5) Bekhof J, Kollen BJ, Groot-Jebbink LJM, et al. Validity and interobserver agreement of reagent strips for measurement of glucosuria. Scand J Clin Lab Investig. 2011; 71(3): 248-52. doi: 10.3109/00365513.2011.558109.
6) Saito Y, Koike J. Color expression by the nursing profession viewed from the perspective of color science. Kitakanto Med J 2001; 51(1): 35-41. doi: 10.2974/kmj.51.35.
7) Sakaguchi M, Saito Y. Examination of the color representation of bloody drainage in a test tube Comparison by years of clinical experience and observation opportunities. J Jpn Soc Nurs Res 1998; 21: 230. doi: 10.15065/jjsnr.19980630153.
8) Japanese Ophthalmological Society. Search by disease name. <https://www.nichigan.or.jp/public/disease/name.html?p-did=33> [cited 2023 Jan 5].
9) Guo D, Li G, Miao JQ, et al. A smartphone-based calibration-free portable urinalysis device. J Central S Univ 2021; 28: 3829-37. doi: 10.1007/s11771-021-4883-7.
10) Woodburn EV, Long KD, Cunningham BT. Analysis of paper-based colorimetric assays with a smartphone spectrometer. IEEE Sens J 2019; 19(2): 508-14. doi: 10.1109/JSEN.2018.2876631.
11) Balbach S, Jiang N, Moreddu R, et al. Smartphone-based colorimetric detection system for portable health tracking. Anal Methods 2021; 13(38): 4361-9. doi: 10.1039/D1AY01209F.
12) Rahmat RF, Royananda, Muchtar MA, et al. Automated color classification of urine dipstick image in urine examination. J Phys Conf Ser 2018; 978: 012008 doi: 10.1088/1742-6596/978/1/012008.
13) Inagaki K. Comparison of judgment results between the color comparison method of urine analysis test papers using the CIE DE2000 color-difference formula and the automatic urine analyzer. J Nurs Sci Eng 2021; 8: 170-6. doi: 10.24462/jnse.8.0_170.
14) Doros G, Lew R. Design based on intra-class correlation coefficients. Am J Biostat 2010; 1(1): 1-8. doi: 10.3844/amjbsp.2010.1.8.
15) Landis JR, Koch GG. The measurement of observer agreement for categorical data. Biometrics 1977; 33(1):

159-74.

16) Tsushima E. Medical data analysis learned in SPSS. Tokyo, Japan: TokyoTosho Co., Ltd. 2016: 212-3.

17) Kim S-C, Cho Y-S. Predictive system implementation to improve the accuracy of urine self-diagnosis with smartphones: Application of a confusion matrix-based learning model through RGB semiquantitative analysis. Sensors 2022; 22 (14) : 5445. doi: 10.3390/s22145445.

18) Ra M, Muhammad MS, Lim C, et al. Smartphone-based point-of-care urinalysis under variable illumination. IEEE J Transl Eng Health Med 2018; 6: 2800111. doi: 10.1109/JTEHM.2017.2765631.

19) Thakur R, Maheshwari P, Datta SK, et al. Machine learning-based rapid diagnostic-test reader for albuminuria using smartphone. IEEE Sens J 2021; 21 (13) : 14011-26. doi: 10.1109/JSEN.2020.3034904.

20) Africa ADM, Velasco JS. Development of a urine strip analyzer using artificial neural network using an android phone. ARPN J Eng Appl Sci 2017; 12 (6) : 1706-13.

21) Siu VS, Lu M, Hsieh KY, et al. Toward a quantitative colorimeter for point-of-care nitrite detection. ACS Omega 2022; 7 (13) : 11126-34. doi: 10.1021/acsomega.1c07205.

22) Healthy.io.
<https://healthy.io/> [cited 2023 Jan 5].

23) Vivoo.
<https://vivoo.io/products/vivoo-urine-test>[cited 2023 Jan 5].

24) Uchek.
<https://www.biosense.in/ucheck.php> [cited 2023 Jan 5].

Original

Evaluation of serum citrullinated fibrinogen in patients with acute aortic dissection

Satoshi Fujimura[*1,2], †Yumiko Higuchi*[*1,3], Atsushi Izawa*[*1,4,5],
Tomoki Ichikawa*[*1], Yoko Usami*[*2], Makoto Yamaura*[*1],
Tsukasa Higuchi*[*6,7], Fumiko Terasawa*[*8], Nobuo Okumura*[*1,3]

†Correspondence: Department of Health and Medical Sciences,Graduate School of Health Sciences Shinshu University 3-1-1 Asahi, Matsumoto 390-8621, Japan.
E-mail: sasa0922@shinshu-u.ac.jp
Received May 26, 2023; accepted March 25, 2024
*1 Department of Health and Medical Sciences, Graduate School of Medicine, Shinshu University, Matsumoto, Japan
*2 Department of Laboratory Medicine, Shinshu University Hospital, Matsumoto, Japan
*3 Department of Biomedical Laboratory Sciences, Shinshu University School of Health Sciences, Matsumoto, Japan
*4 Department of Nursing, Shinshu University School of Medicine, Matsumoto, Japan
*5 Department of Cardiovascular Medicine, Shinshu University School of Health Sciences, Matsumoto, Japan
*6 Department of General Pediatrics, Nagano Children's Hospital, Azumino, Japan
*7 Life Science Research Center, Nagano Children's Hospital, Azumino, Japan
*8 Faculty of Health and Medical Sciences, Department of Medical Technology and Clinical Engineering, Hokuriku University, Kanazawa, Japan

ABSTRACT

Background: Acute aortic dissection (AAD) is a life-threatening cardiovascular disease that requires rapid intervention. The present study assessed the serum citrullinated fibrinogen (C-Fbg) levels in patients with AAD and investigated their clinical utility.
Materials and methods: Serum C-Fbg concentrations were measured at the first blood sample of AAD patients (n = 34) and compared with those of healthy controls (HCs; n = 23) and patients with ischemic heart disease (IHD; n = 10). We also assessed the correlations between C-Fbg levels and inflammatory and coagulation markers in patients with early-phase AAD as well as the time course of these markers, including C-Fbg.
Results: Serum C-Fbg levels were significantly higher in AAD patients than in HCs ($p<0.001$) and IHD patients ($p<0.01$), and serum C-Fbg levels correlated with D-dimer but not with other markers. Receiver operating characteristic (ROC) curve analysis revealed that C-Fbg concentrations were effective in differentiating AAD from IHD. In contrast to the decrease in D-dimer levels, C-Fbg concentrations remained high and relatively unchanged in early-phase AAD.
Conclusion: Serum C-Fbg levels were elevated in patients with AAD, and could differentiate AAD from IHD. Although further studies are needed, C-Fbg may be an adjunctive tool in the differential diagnosis of AAD.
〔Lab Med Int 2024; 3(2): 50-58〕

Key Words
Citrullinated fibrinogen, Acute aortic dissection, Ischemic heart disease, D-dimer

I. Introduction

Acute aortic dissection (AAD) is a life-threatening cardiovascular disease associated with high mortality [1], and early diagnosis is required to improve its prognosis. Although there are still uncertainties concerning the mechanisms underlying the onset of aortic dissection [2], many studies have demonstrated that a certain level

of inflammation involving neutrophil or macrophage infiltration into aortic tissue is associated with the formation of aortic dissection [1) 3)-8)].

The diagnosis of AAD is primarily based on symptoms and imaging findings. Blood tests play a role in the acute setting and can enhance the differential diagnosis of AAD from other serious illnesses. Many biochemical assays have been developed to detect AAD in such patients [9)10)], including evaluations of smooth muscle myosin [11)], matrix metalloproteinase-9 [12)], elastin degradation products [13)], calponin [14)], transforming growth factor-beta[15)] and D-dimer [16) 17)]. Among them, serum D-dimer concentration is currently the only biomarker for distinguishing AAD from ischemic heart disease (IHD) in the clinical settings [18) 19)]. Therefore, other rapid and accurate biomarkers are needed to enhance the diagnosis of AAD in the acute phase.

Protein citrullination involves the posttranslational modification of arginine to citrulline via the calcium-dependent enzyme peptidylarginine deiminase (PAD) [20)21)]. The 5 PAD isozymes (PAD 1, 2, 3, 4, and 6) are tissue-specifically distributed in human body and citrullinate proteins in a substrate-specific manner [22)]. Among them, PAD2 and PAD4 are expressed in blood cells [23)].

Citrullinated proteins have been investigated as antigens for autoimmune antibodies in rheumatoid arthritis [20) 21)]. Among them, citrullinated fibrinogen (C-Fbg) is a well-known candidate autoantigen abundant in the joints of patients with rheumatoid arthritis, where a complicated inflammatory response occurs[24)]. However, little is known about the physiological or pathological role of C-Fbg in other diseases.

We previously showed that C-Fbg levels were increased in patients with bacteremia, which was correlated with neutrophilia[25)]. As neutrophilia is detected soon after AAD occurs [26)], we hypothesized that Fbg might be citrullinated by PAD derived from increased neutrophils in or around the aortic wall in patients with AAD, causing an increase in C-Fbg levels.

In the present study, we assessed the specificity and potential clinical use of C-Fbg as an acute-phase marker for the early diagnosis of patients with suspected AAD.

II. Materials and methods

Subjects

Patients enrolled in this study were admitted to the Advanced Emergency and Critical Care Center of Shinshu University Hospital from November 2017 to July 2018 and diagnosed with AAD (Stanford type A or B) and IHD (7 cases of acute myocardial infarction, 2 cases of angina, and 1 case of acute coronary syndrome). Patients diagnosed with an infectious disease or active autoimmune disease, such as rheumatoid arthritis or systemic lupus erythematosus, were excluded. In this study, 1–6 serum samples were obtained from 34 patients with AAD (n = 118) and 10 patients with IHD (n = 10) independent of treatment strategy. For healthy controls (HCs; n = 23), blood samples were obtained from healthy volunteers after informed consent was obtained. All serum samples were stored at -30℃ until analysis. Clinical laboratory data, including concentrations of C-reactive protein (CRP), Fbg, and D-dimer, complete blood count, and differential white blood cell counts, were collected from the patients' medical records. The reference intervals of values at Shinshu University Hospital were used. The participants' detailed information is provided in **Table 1**.

This study was conducted in accordance with The Code of Ethics of the World Medical Association (Declaration of Helsinki) and approved by the Ethical Review Board of Shinshu University School of Medicine (no. 3928).

Sandwich enzyme-linked immunosorbent assay for C-Fbg

C-Fbg was quantified using a sandwich enzyme-linked immunosorbent assay method that we previously established. Briefly, the generated anti-C-Fbg antibody (clone F) was used as a precoating antibody, while biotin-conjugated anti-Fbg polyclonal antibody (Ab6666; Abcam, Cambridge, UK) was used as the secondary antibody [25)].

The synthesis, purification, and citrullination of recombinant fibrinogen used as a standard were described previously [27)-29)].

Statistical analyses

All statistical analyses were performed using EZR software (Saitama Medical Center, Jichi Medical University, Saitama, Japan), a graphical user interface for R software (The R Foundation for Statistical Computing, Vienna, Austria). The Mann–Whitney U test was used to compare inflammatory and coagulation markers between patients with AAD and those with IHD. In addition, a receiver operating characteristic (ROC) curve analysis was performed for C-Fbg concentration in patients with AAD and IHD. The optimal cut-off value was determined using Youden's index. The Kruskal–Wallis test with the Steel–Dwass test was also used to compare C-Fbg concentrations between patients with AAD and those with IHD in the first submission sample and the HCs, as were chronological changes in C-Fbg and other markers. Moreover, the time-course transition of C-Fbg level and neutrophil count was evaluated using the same statistical analysis. Spearman's rank correlation test was used

Table 1 Clinical characteristics of the patients and healthy controls

	Healthy controls		AAD patients		IHD patients		
	Median (IQR)	n	Median (IQR)	n	Median (IQR)	n	*p*
Age, years	51.0 (44.5-60.0)	23	74.5 (67.0-80.8)	34	76.5 (71.3-78.5)	10	
Sex (male/female)		10/13		17/17		6/4	
Laboratory tests							
Neutrophil (× 10^3) (/μL)	NA		8.2 (6.3-11.6)	31	6.0 (4.6-7.6)	9	<0.05
PLT (× 10^3) (/μL)	NA		166.0 (144.5-204.0)	34	159.0 (146.5-208.3)	10	0.944
CRP (mg/L)	NA		1.3 (0.3-3.3)	34	0.8 (0.5-2.5)	10	1.000
Fbg (g/L)	NA		2.4 (1.8-2.9)	33	2.9 (2.6-3.0)	10	0.182
D-dimer (μg/mL)	NA		15.7 (5.4-40.8)	34	0.8 (0.6-1.7)	10	<0.001
Classification of AAD							
Stanford type A (DeBakey I / II)				25 (17/8)			
Surgical treatment				21			
Conservative treatment				4			
Stanford type B				9			
Surgical treatment				0			
Conservative treatment				9			
Classification of IHD							
Acute myocardial infarction						7	
Angina						2	
Acute coronary syndrome						1	

AAD: acute aortic dissection, CRP: C-reactive protein, Fbg: fibrinogen. IHD: IHD: ischemic heart disease, IQR: interquartile range, NA: not analyzed, PLT: platelet count.

to determine the correlation between serum C-Fbg level and other clinical factors. P values < 0.05 were considered statistically significant.

III. Results

Initial serum C-Fbg concentrations of patients with AAD versus IHD

First, we evaluated the serum C-Fbg concentration in the first submitted sample of patients with AAD and compared them to those of patients with IHD and HCs. As illustrated in **Figure 1A**, the serum C-Fbg level in the first sample of AAD patients (median [range], 153.8 [101.2–218.6] ng/mL) was significantly higher than those of IHD patients (83.1 [74.0–92.9] ng/mL; $p < 0.01$) and HCs (40.5 [31.5–50.6] ng/mL; $p < 0.001$). A significant difference was also observed in the C-Fbg concentrations between the IHD patients and HCs. There were no significant differences in C-Fbg concentration between the cases of Stanford type A and B (**Figure 1B**) or DeBakey I and II (data not shown) in the AAD group.

The ROC analysis of C-Fbg concentrations in AAD and IHD patients in the first samples revealed an area under the curve (AUC) of 0.821 (95% confidence interval, 0.667–0.974) with a cut-off value of 94.1 ng/mL, sensitivity of 80.0%, and specificity of 82.4% (**Figure 1C**).

Initial inflammatory and coagulation marker levels of patients with AAD versus IHD

Next, we compared the initial inflammatory and coagulation marker levels (neutrophil count, platelet count [PLT], CRP, Fbg, and D-dimer) of patients with AAD and IHD (**Table 1**). The neutrophil counts were significantly higher in the AAD group (8.2 [6.3–11.6] × 10^3/μL) than in the IHD group (6.0 [4.6–7.6] × 10^3/μL, $p<0.05$). The D-dimer values in the AAD group (15.7 [5.4–40.8] μg/mL) were also significantly higher than those in the IHD group (0.8 [0.6–1.7] μg/mL; $p < 0.001$), as reported by other researchers [30)-32)]. There were no significant intergroup differences in PLT ($p = 0.944$), CRP ($p = 1.000$), or Fbg ($p = 0.182$).

We also assessed whether C-Fbg concentration was related to the initial neutrophil count and D-dimer, PLT, CRP, or Fbg values of the AAD group. C-Fbg showed a moderately positive correlation with D-dimer ($r = 0.443$, $p < 0.01$; **Figure 2B**), but it was not correlated with neutrophil count ($r = 0.186$, $p = 0.315$; **Figure 2A**), PLT ($r = 0.256$, $p = 0.145$; **Figure 2C**), CRP ($r = 0.164$, $p = 0.355$; **Figure 2D**), or Fbg ($r = -0.08$, $p = 0.657$; **Figure 2E**).

Time course of C-Fbg and other markers

Our previous study revealed that serum C-Fbg levels were increased in patients with bacteremia, consistent with the influx of neutrophils into the bloodstream in

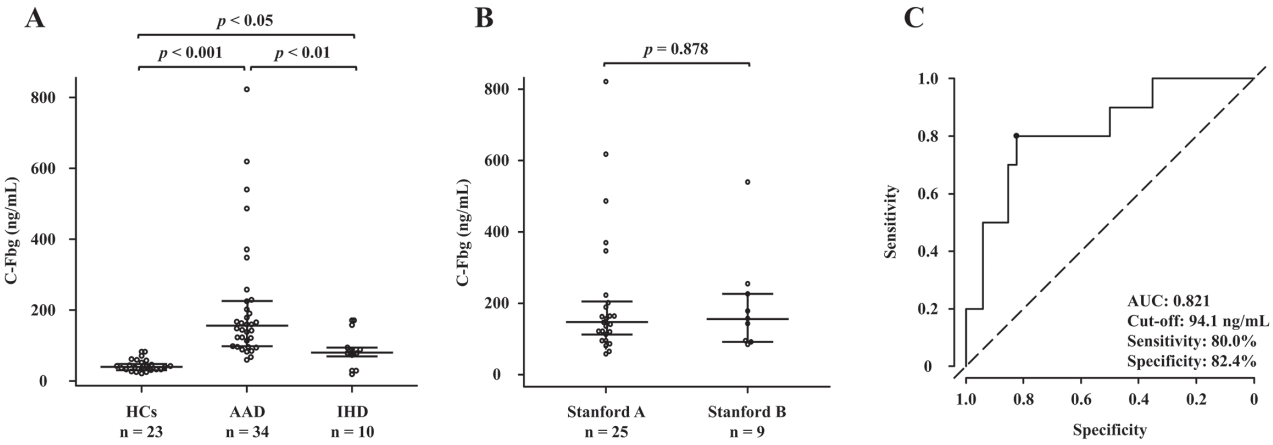

Figure 1 Serum C-Fbg concentrations and ROC analysis results. Initial levels measured of the (A) HCs (n = 23), AAD patients (n = 34), and IHD patients (n = 10). (B) Levels in patients with Stanford type A and B AAD were compared. The bar indicates median and interquartile range. The statistical analysis was performed using the Kruskal–Wallis and Steel–Dwass test (A) and the Mann–Whitney U test (B). (C) The ROC analysis of the initial serum C-Fbg level of AAD versus IHD patients is shown. AAD, acute aortic dissection; C-Fbg, citrullinated fibrinogen; HCs, healthy controls; IHD, ischemic heart disease; ROC, receiver operating characteristic

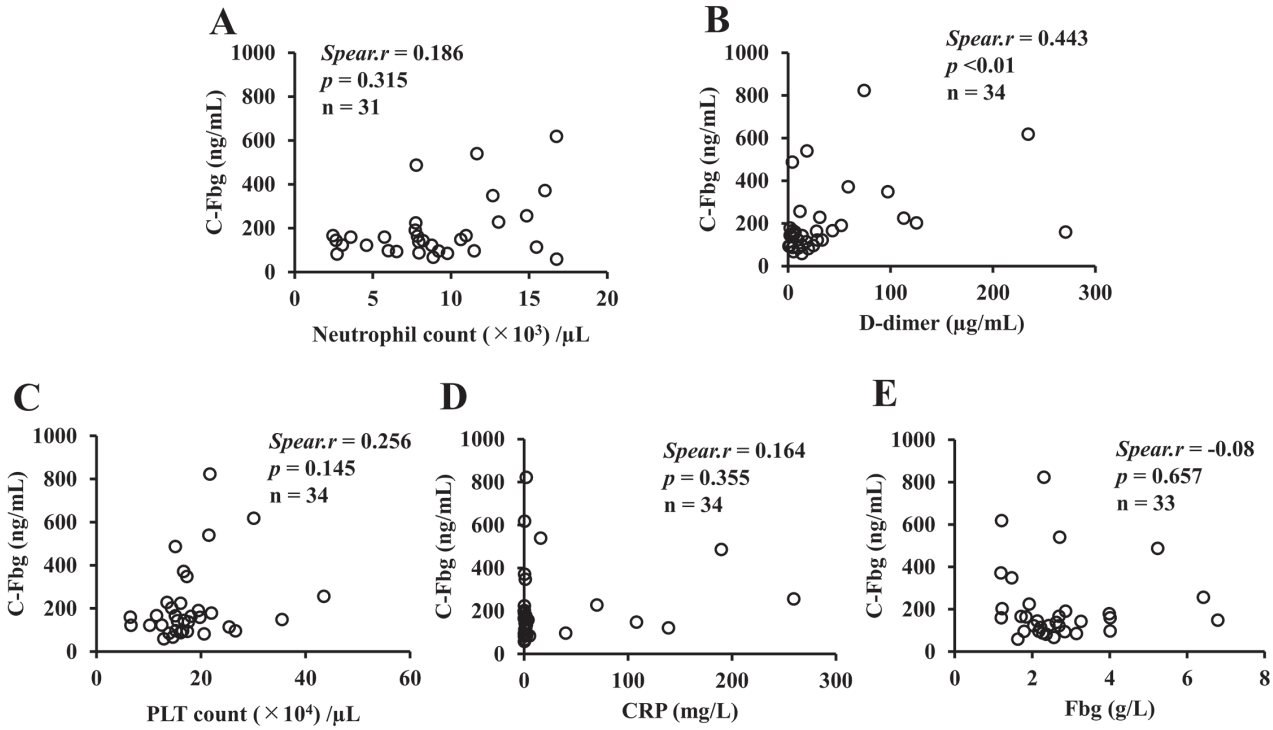

Figure 2 Correlation between C-Fbg concentration and inflammatory markers in the initial sample taken from patients with AAD. The correlations between C-Fbg and neutrophil count (A), D-dimer (B), PLT count (C), CRP level (D), and Fbg concentration (E) are shown. The significance of the correlation (p) was analyzed with Spearman's rank correlation coefficient (*Spear. r*). AAD, acute aortic dissection; C-Fbg, citrullinated fibrinogen; CRP, C-reactive protein; Fbg, fibrinogen; PLTc platelet count

accordance with the bacteremia phase [25]. Thus, we assessed the time course of C-Fbg and neutrophil count after AAD patient admission as well as the correlation between C-Fbg and neutrophil count. We also compared the time course of C-Fbg with that of D-dimer, CRP, and Fbg levels. Clinical data of neutrophil counts, D-dimer, CRP, and Fbg along with C-Fbg concentration in the time-course analyses were available for 23 of the 34 AAD patients. The values were classified according to sample submission timing after the patients were admitted: 0 h (initial sample), 1–24 h, 25–48 h, 49–72 h, and 73–96 h.

The C-Fbg concentration in AAD patients remained high compared to that of HCs and remained relatively unchanged until 73–96 h (**Figure 3A**). The mean

neutrophil count remained above the normal range throughout the time course. Aortic dissection promotes rapid mobilization of neutrophils to the adventitia of the dissected aorta, and the value peaks at 12–24 h after the event [8]. As the half-life of neutrophils is <24 h [33], our results suggest the involvement of continuous neutrophil recruitment from the bone marrow in response to aortic dissection (**Figure 3B**). However, we detected no correlation between C-Fbg level and neutrophil count in any of the classified phases (**Figure 4**).

The time course of D-dimer, CRP, and Fbg levels demonstrated characteristic transitions from 0 to 96 h after the onset of AAD (**Figure 3**). D-dimer levels peaked at 0 h and then decreased rapidly within 48 h (**Figure 3C**). CRP levels began to increase at 1–24 h and peaked at 49–72 h (**Figure 3D**). Fbg showed a continuous increase after 25 h until 73–96 h (**Figure 3E**).

Discussion

In the present study, serum C-Fbg concentrations in patients with AAD were analyzed and compared with the inflammatory and coagulation markers.

We clarified that the initial serum C-Fbg concentrations of AAD patients were significantly higher than those of HCs and IHD patients. Furthermore, there were no significant differences in C-Fbg concentration between the cases of Stanford type A and B or DeBakey I and II in the AAD group. Generally, Stanford type A is considered as more severe condition than type B because of its involvement in ascending aortic dissection [34]. Stanford type A is further classified DeBakey I (dissection of the entire aorta) and II (dissection of the ascending aorta only), and former is severe than latter [34]. Thus, this might suggest that severity of the illness had no effect on the C-Fbg concentration. The neutrophil counts in the AAD group were also significantly higher than those

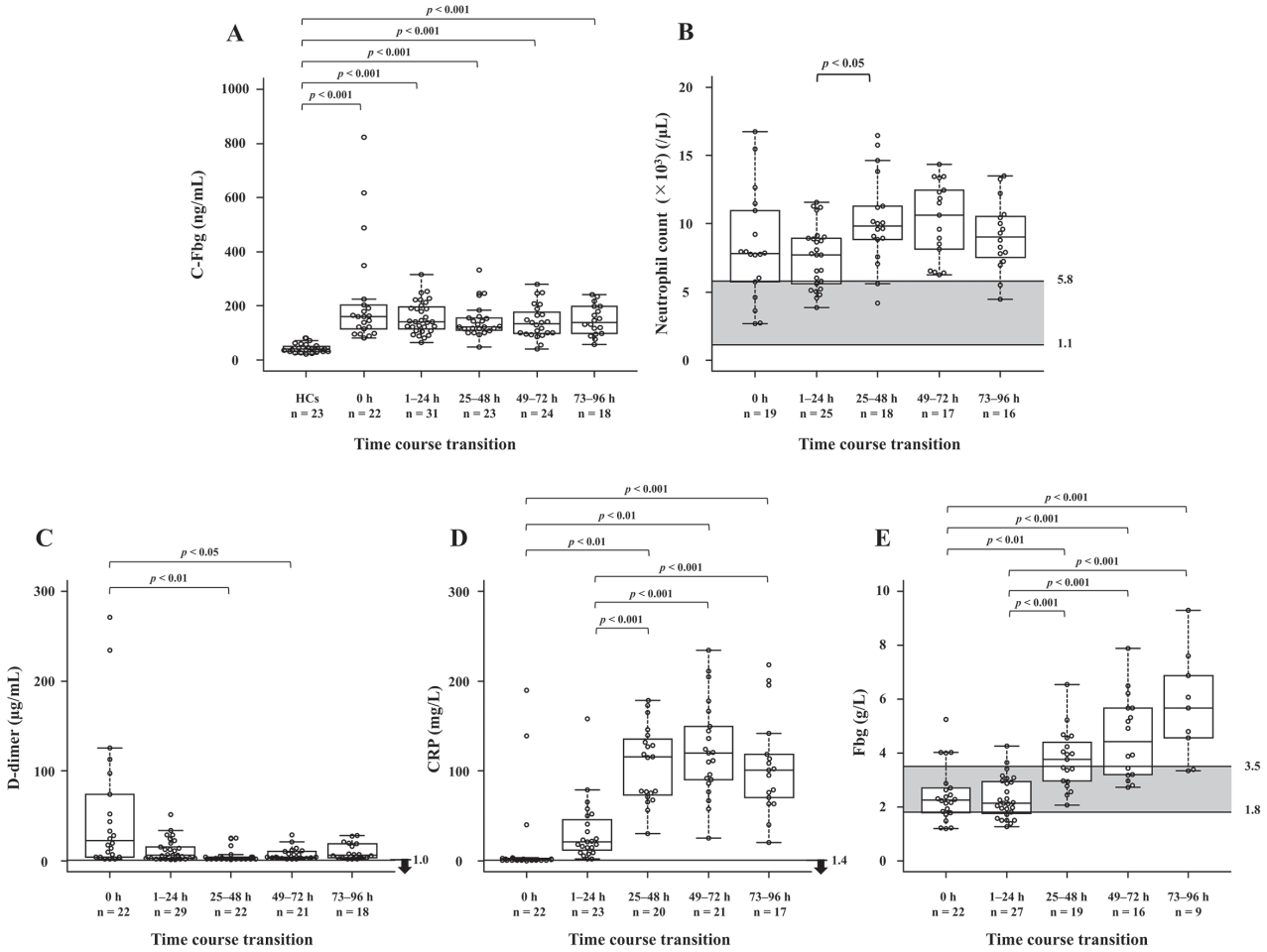

Figure 3 Time course of C-Fbg and other inflammatory markers. Samples from 23 AAD patients were classified by the submission time; 0 h (the first submission sample), 1-24 h, 25-48 h, 49-72 h, 73-96 h. The concentration of serum C-Fbg (A), neutrophil counts (B), and concentrations of D-dimer (C), CRP (D), and Fbg (E) are shown. The bar indicates the medians with the interquartile range. The reference interval of each marker at Shinshu University Hospital is depicted by a gray area or bar and arrow. The statistical analyses were performed by the Kruskal–Wallis and Steel–Dwass test. AAD, acute aortic dissection; C-Fbg, citrullinated fibrinogen; CRP, C-reactive protein; Fbg, fibrinogen; HCs, healthy controls

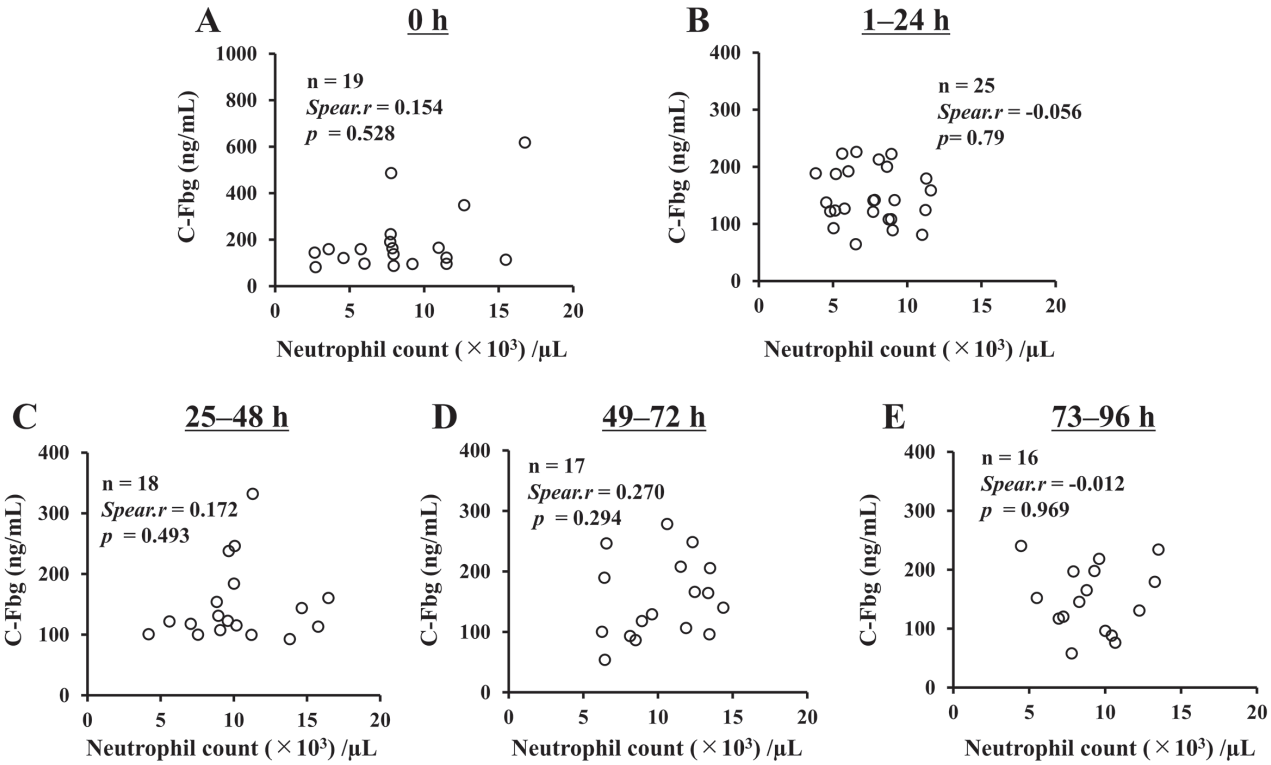

Figure 4 Correlation between C-Fbg concentration and neutrophil count in the sample of patients with AAD at each classified phase as follows: 0 h (initial sample) (A), 1–24 h (B), 25–48 h (C), 49–72 h (D), and 73–96 h (E) after admission. The significance of the correlation (p) was analyzed with Spearman's rank correlation coefficient (*Spear. r*).
AAD, acute aortic dissection; C-Fbg, citrullinated fibrinogen

in the IHD group. Our previous report demonstrated that the C-Fbg concentration increased in bacteremia patients consistent with the influx of neutrophils into the bloodstream in accordance with the bacteremia phase [25]. The increase in C-Fbg levels was induced by increased PAD derived from activated neutrophils in patients with bacteremia. Therefore, we hypothesized that C-Fbg in AAD patients is also generated by PAD from activated neutrophils, so the C-Fbg concentration would increase along with neutrophilia in AAD patients.

The estimated half-life of C-Fbg in vivo is approximately 2.5–3.5 days, which is similar to that of fibrinogen (2-4 days) [35]. Our data showed that C-Fbg concentrations in AAD patients remained high through the time course compared to that of HCs from the first submission to 73–96 h. Moreover, there were no significant differences in C-Fbg levels at any time point between patients with and without surgical intervention (data not shown). This suggested that C-Fbg in patients was continuously generated through at least 96 h after AAD onset, and it represented sustained inflammatory responses until 73–96 h with or without surgery. However, there was no correlation between C-Fbg concentration and peripheral blood neutrophil count throughout the time course.

Interestingly, a recent study revealed that neutrophil extracellular traps (NETs) are involved in AAD [36) 37)]. NETs, consisting of intracellular substances such as enzymes, proteins, and DNA, are released extracellularly by neutrophils and play a critical role in inflammatory processes [38)]. The presence of NETs in the aortic tissues and serum of patients with thoracic aortic dissection and its mouse model has been proven [37)]. Other investigators also demonstrated that NET components may constitute useful diagnostic and prognostic markers in patients with AAD [36)]. PAD is also released from neutrophils as a NET component and citrullinates many kinds of plasma proteins [39) 40)]. Thus, we hypothesized that the source of PAD, inducing the citrullination of Fbg, is probably activated neutrophils and macrophages that infiltrate the inflammatory site. Pathologically, aortic dissection is characterized by dissection of the aortic media. Recent studies in mouse models of aortic dissection have shown that inflammatory cells, such as macrophages and granulocytes, are involved in the onset of aortic dissection [12) 41)]. In a human study, the initial influx of neutrophils into the adventitia occurred within hours of the onset of pain, followed by a peak at 12–24 h and a gradual decrease that persisted for 2–7 days [8)]. These infiltrated and activated blood cells potentially produce and release PAD, leading to the citrullination of Fbg.

Therefore, peripheral blood neutrophil counts did not necessarily correlate with the amount of PAD released or the C-Fbg concentration in contrast to patients with bacteremia.

There is another explanation for this discrepancy between serum C-Fbg concentrations and peripheral neutrophil counts. PAD2, an isoform of PAD, is also present in the aorta at the mRNA level according to the expressed sequence tag database [42]. Therefore, the release of PAD2 from the injured aortic wall via mechanical stimulation or inflammatory molecules upon aortic dissection may induce the citrullination of Fbg. In this case, neutrophils are not necessarily correlated with C-Fbg because they are not its main source.

Next, we analyzed the relationship between C-Fbg concentration and D-dimer, Fbg, and CRP levels. As shown in **Figure 3C**, D-dimer levels rapidly increased at AAD onset as generally reported [30) 43)] and peaked earlier than those of CRP and Fbg. C-Fbg also rapidly increased at AAD onset, and the levels were correlated with those of D-dimer, but not with other markers. In addition, our results showed that the C-Fbg concentration in the AAD group was significantly higher than that in the IHD group. As the most common symptom of AAD is sudden-onset severe chest or back pain [10], physicians often need to distinguish AAD from IHD. In an acute setting, D-dimer is currently the only commercially available test for reinforcing the biochemical diagnosis of aortic dissection. Although the sensitivity is high (96.6%) with a D-dimer cut-off of 0.5 μg/mL to rule out clinically suspected AAD, the specificity is low (46.6%) [2]. Our results showed that ROC curve analysis further revealed the utility of C-Fbg for distinguishing between AAD and IHD (AUC, 0.821; 95% confidence interval, 0.667–0.974) by using a C-Fbg with a cut-off value of 94.1 ng/mL (sensitivity, 80.0%; specificity, 82.4%). Thus, serum C-Fbg may be a potentially useful clinical adjunctive AAD biomarker in patients presenting with acute-onset severe chest or back pain. In addition, D-dimer levels decreased significantly 25 h after AAD onset, while C-Fbg levels remained elevated until 96 h. Therefore, the difference in kinetics between C-Fbg and D-dimer may aid the accurate AAD diagnosis, especially after 25 hours post-onset.

Some limitations of the present study warrant mentioning. First, because of its small sample size, we could not conduct detailed analyses according to classification or known risk factors for aortic dissection. Second, this is a retrospective study with limited samples and information, so that prospective study is needed to evaluate clinical utility of C-Fbg in AAD further. Third, the samples were obtained independently of any treatment of AAD. We confirmed surgery did not affect C-Fbg concentration, but we could not exclude the possibility that drug treatment might influence C-Fbg production in patients with AAD. Forth, we did not analyze the relationship between C-Fbg and AAD prognosis. Many factors have been reported as prognostic markers in AAD [44)-47)]. It will be very interesting to see if C-Fbg can be used as diagnostic and prognostic marker in AAD.

In conclusion, this is the first report to demonstrate an initially increased serum C-Fbg concentrations among patients with AAD. Our results indicate that C-Fbg may be a useful adjunctive differential diagnostic tool for AAD. As the physiological or pathological role of C-Fbg has not been evaluated in AAD, further investigations are needed to determine the clinical utility of C-Fbg, especially in cardiovascular emergencies.

Funding

This work was supported by the Charitable Trust Laboratory Medicine Research Foundation of Japan [2019] and JSPS KAKENHI (no. JP20K07822).

Authorship Contributions

YH, AI, TH, NO, and SF designed the study and prepared the manuscript. SF, TI, YH, and FT performed the experiments and analyzed the data. TI, YU, MY, YH, and SF collected the samples and data. All authors have read and approved the final version of the manuscript.

Disclosure of Conflicts of Interest

All authors declare no conflicts of interest.

References

1) Luo F, Zhou XL, Li JJ, et al. Inflammatory response is associated with aortic dissection. Ageing Res Rev 2009; 8(1):31-5. doi: 10.1016/j.arr.2008.08.001.

2) Ogino H, Iida O, Akutsu K, et al. JCS/JSCVS/JATS/JSVS Guideline on Diagnosis and Treatment of Aortic Aneurysm and Aortic Dissection. 2020. (in Japanease) Available from: URL: https://www.j-circ.or.jp/cms/wp-content/uploads/2020/07/JCS2020_Ogino.pdf (Accessed December 24, 2022).

3) Cifani N, Proietta M, Tritapepe L, et al. Stanford-A acute aortic dissection, inflammation, and metalloproteinases: A review. Ann Med 2015; 47(6):441-6. doi: 10.3109/07853890.2015.1073346.

4) Niinimäk E, Pynnönen V, Kholova I, et al. Neovascularization with chronic inflammation characterizes ascending

aortic dissection. Anatol J Cardiol 2018; 20(5):289-95. doi: 10.14744/AnatolJCardiol.2018.42223.

5) Wu D, Choi JC, Sameri A, et al. Inflammatory cell infiltrates in acute and chronic thoracic aortic dissection. Aorta (Stamford) 2013; 1(6): 259-67. doi: 10.12945/j.aorta.2013.13-044.

6) Son BK, Sawaki D, Tomida S, et al. Granulocyte macrophage colony-stimulating factor is required for aortic dissection/intramural haematoma. Nat Commun 2015; 6: 6994. doi: 10.1038/ncomms7994.

7) Anzai A, Shimoda M, Endo J, et al. Adventitial CXCL1/G-CSF expression in response to acute aortic dissection triggers local neutrophil recruitment and activation leading to aortic rupture. Circ Res 2015; 116(4):612-23. doi: 10.1161/CIRCRESAHA.116.304918.

8) Xu L, Burke A. Acute medial dissection of the ascending aorta: Evolution of reactive histologic changes. Am J Surg Pathol 2013; 37(8):1275-82. doi: 10.1097/PAS.0b013e318294adc3.

9) Wen D, Zhou XL, Li JJ, Hui RT. Biomarkers in aortic dissection. Clin Chim Acta. 2011; 412(9-10):688-95. doi: 10.1016/j.cca.2010.12.039.

10) Nienaber CA, Clough RE. Management of acute aortic dissection. Lancet 2015; 385(9970):800-11. doi: 10.1016/s0140-6736(14)61005-9.

11) Katoh H, Suzuki T, Yokomori K, et al. A novel immunoassay of smooth muscle myosin heavy chain in serum. J Immunol Methods 1995; 185(1): 57-63. doi: 10.1016/0022-1759(95)00104-i.

12) Kurihara T, Shimizu-Hirota R, Shimoda M, et al. Neutrophil-derived matrix metalloproteinase 9 triggers acute aortic dissection. Circulation 2012; 126(25): 3070-80. doi: 10.1161/circulationaha.112.097097.

13) Shinohara T, Suzuki K, Okada M, et al. Soluble elastin fragments in serum are elevated in acute aortic dissection. Arterioscler Thromb Vasc Biol 2003; 23(10): 1839-44. doi: 10.1161/01.Atv.0000085016.02363.80.

14) Suzuki T, Distante A, Zizza A, et al. Preliminary experience with the smooth muscle troponin-like protein, calponin, as a novel biomarker for diagnosing acute aortic dissection. Eur Heart J 2008; 29(11): 1439-45. doi: 10.1093/eurheartj/ehn162.

15) Suzuki T, Trimarchi S, Sawaki D, et al. Circulating transforming growth factor-beta levels in acute aortic dissection. J Am Coll Cardiol 2011; 58(7): 775. doi: 10.1016/j.jacc.2010.01.079.

16) Akutsu K, Sato N, Yamamoto T et al. A rapid bedside D-dimer assay (cardiac D-dimer) for screening of clinically suspected acute aortic dissection. Circ J 2005; 69(4): 397-403. doi: 10.1253/circj.69.397.

17) Weber T, Högler S, Auer J, et al. D-dimer in acute aortic dissection. Chest 2003; 123(5): 1375-8. doi: 10.1378/chest.123.5.1375.

18) Sodeck G, Domanovits H, Schillinger M, et al. D-dimer in ruling out acute aortic dissection: A systematic review and prospective cohort study. Eur Heart J 2007; 28(24): 3067-75. doi: 10.1093/eurheartj/ehm484.

19) Zhang B, Wang Y, Guo J, et al. Nomogram to differentiate between aortic dissection and non-ST segment elevation acute coronary syndrome: a retrospective cohort study. Cardiovasc Diagn Ther 2021; 11(2): 457-66. doi: 10.21037/cdt-20-935.

20) Valesini G, Gerardi MC, Iannuccelli C, et al. Citrullination and autoimmunity. Autoimmun Rev 2015; 14(6): 490-7. doi: 10.1016/j.autrev.2015.01.013.

21) György B, Tóth E, Tarcsa E, et al. Buzás EI. Citrullination: a posttranslational modification in health and disease. Int J Biochem Cell Biol 2006; 38(10): 1662–77. doi: 10.1016/j.biocel.2006.03.008.

22) Chavanas S, Méchin MC, Takahara H, et al. Comparative analysis of the mouse and human peptidylarginine deiminase gene clusters reveals highly conserved non-coding segments and a new human gene, PADI6. Gene 2004; 330: 19-27. doi: 10.1016/j.gene.2003.12.038.

23) Mohanan S, Cherrington BD, Horibata S, et al. Potential role of peptidylarginine deiminase enzymes and protein citrullination in cancer pathogenesis. Biochem Res Int 2012; 2012: 895343. doi: 10.1155/2012/895343.

24) Wegner N, Lundberg K, Kinloch A, et al. Autoimmunity to specific citrullinated proteins gives the first clues to the etiology of rheumatoid arthritis. Immunol Rev 2010; 233(1): 34-54. doi: 10.1111/j.0105-2896.2009.00850.x.

25) Fujimura S, Higuchi Y, Usami Y, et al. Changes in serum citrullinated fibrinogen concentration associated with the phase of bacteremia patients. Clin Chim Acta 2021; 512: 127-34. doi: 10.1016/j.cca.2020.10.038.

26) Zhang J, Jiang Y, Gao C, et al. Risk factors for hospital death in patients with acute aortic dissection. Heart Lung Circ 2015; 24(4): 348-53. doi: 10.1016/j.hlc.2014.10.009.

27) Okumura N, Haneishi A, Terasawa F. Citrullinated fibrinogen shows defects in FPA and FPB release and fibrin polymerization catalyzed by thrombin. Clin Chim Acta. 2009; 401(1-2):119–23. doi: 10.1016/j.cca.2008.12.002.

28) Hirota-Kawadobora M, Kani S, Terasawa F, et al. Functional analysis of recombinant Bbeta15C and Bbeta15A fibrinogens demonstrates that Bbeta15G residue plays important roles in FPB release and in lateral aggregation of protofibrils. J Thromb Haemost 2005; 3(5): 983–90. doi: 10.1111/j.1538-7836.2005.01294.x.

29) Terasawa F, Ishii W, Higuchi Y, et al. Measurement of the

serum levels of citrullinated fibrinogen and its antibodies in rheumatoid arthritis patients. Int J Anal Bio-Sci 2016; 39(4): 263–70. (in Japanease)

30) Suzuki T, Distante A, Zizza A, et al. Diagnosis of acute aortic dissection by D-dimer: the International Registry of Acute Aortic Dissection Substudy on Biomarkers (IRAD-Bio) experience. Circulation 2009; 119(20): 2702-7. doi: 10.1161/CIRCULATIONAHA.108.833004.

31) Ohlmann P, Faure A, Morel O, et al. Diagnostic and prognostic value of circulating D-Dimers in patients with acute aortic dissection. Crit Care Med 2006; 34(5): 1358-64. doi: 10.1097/01.Ccm.0000216686.72457.Ec.

32) Hazui H, Fukumoto H, Negoro N, et al. Simple and useful tests for discriminating between acute aortic dissection of the ascending aorta and acute myocardial infarction in the emergency setting. Circ J 2005; 69(6): 677-82. doi: 10.1253/circj.69.677.

33) Lahoz-Beneytez J, Elemans M, Zhang Y, et al. Human neutrophil kinetics: Modeling of stable isotope labeling data supports short blood neutrophil half-lives. Blood 2016; 127(26): 3431-8. doi: 10.1182/blood-2016-03-700336.

34) Tsai TT, Nienaber CA, Eagle KA. Acute aortic syndromes. Circulation 2005; 112(24): 3802-13. doi: 10.1161/CIRCULATIONAHA.105.534198.

35) Mannucci PM, Duga S, Peyvandi F. Recessively inherited coagulation disorders. Blood 2004; 104(5): 1243-52. doi: 10.1182/blood-2004-02-0595.

36) Yang S, Xiao Y, Du Y, et al. Diagnostic and Prognostic Value of Neutrophil Extracellular Trap Levels in Patients With Acute Aortic Dissection. Front Cardiovasc Med 2021; 8: 683445. doi: 10.3389/fcvm.2021.683445.

37) Pan G, Liao M, Dai Y, et al. Inhibition of sphingosine-1-phosphate receptor 2 prevents thoracic aortic dissection and rupture. Front Cardiovasc Med 2021; 8: 748486. doi: 10.3389/fcvm.2021.748486.

38) Brinkmann V, Reichard U, Goosmann C, et al. Neutrophil extracellular traps kill bacteria. Science 2004; 303(5663): 1532–5. doi: 10.1126/science.1092385.

39) Hasler P, Giaglis S, Hahn S. Neutrophil extracellular traps in health and disease. Swiss Med Wkly 2016; 146: w14352. doi: 10.4414/smw.2016.14352.

40) Darrah E, Andrade F. Rheumatoid arthritis and citrullination. Curr Opin Rheumatol 2018; 30(1): 72-8. doi: 10.1097/bor.0000000000000452.

41) Tomida S, Aizawa K, Nishida N, et al. Indomethacin reduces rates of aortic dissection and rupture of the abdominal aorta by inhibiting monocyte/macrophage accumulation in a murine model. Sci Rep 2019; 9(1): 10751. doi: 10.1038/s41598-019-46673-z.

42) Vossenaar ER, Zendman AJ, van Venrooij WJ, et al. PAD, a growing family of citrullinating enzymes: Genes, features and involvement in disease. BioEssays 2003; 25(11): 1106-18. doi: 10.1002/bies.10357.

43) Peng W, Peng Z, Chai X, et al. Potential biomarkers for early diagnosis of acute aortic dissection. Heart Lung 2015; 44(3): 205-8. doi: 10.1016/j.hrtlng.2015.01.006.

44) Karakoyun S, Gürsoy MO, Akgün T, et al. Neutrophil-lymphocyte ratio may predict in-hospital mortality in patients with acute type A aortic dissection. Herz 2015; 40(4): 716-21. doi: 10.1007/s00059-014-4121-2.

45) Oz K, Iyigun T, Karaman Z, et al. Prognostic Value of neutrophil to lymphocyte ratio and risk factors for mortality in patients with Stanford type A aortic Dissection. Heart Surg Forum 2017; 20(3): E119-23. doi: 10.1532/hsf.1736.

46) Onuk T, Güngör B, Karataş B, et al. increased neutrophil to lymphocyte ratio is associated with in-hospital mortality in patients with aortic dissection. Clin Lab 2015; 61(9): 1275-82.

47) Li S, Yang J, Dong J, et al. Neutrophil to lymphocyte ratio and fibrinogen values in predicting patients with type B aortic dissection. Sci Rep 2021; 11(1): 11366. doi: 10.1038/s41598-021-90811-5.